The examples of degree of pozzolanic reaction of low and high calcium fly ashes in the pastes with w/b of 0.40 and f/b of 0.30 used in this model are shown in Fig. 2 [15]

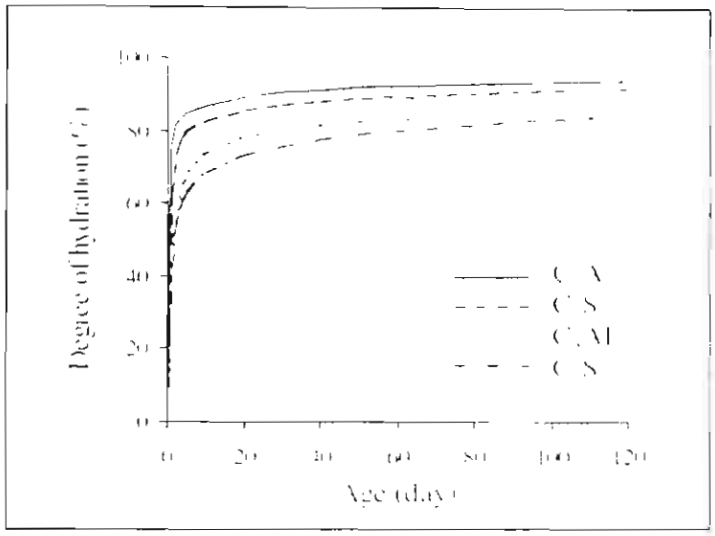

Fig. 1 Example of degree of hydration of type I cement (w/c=0.40)

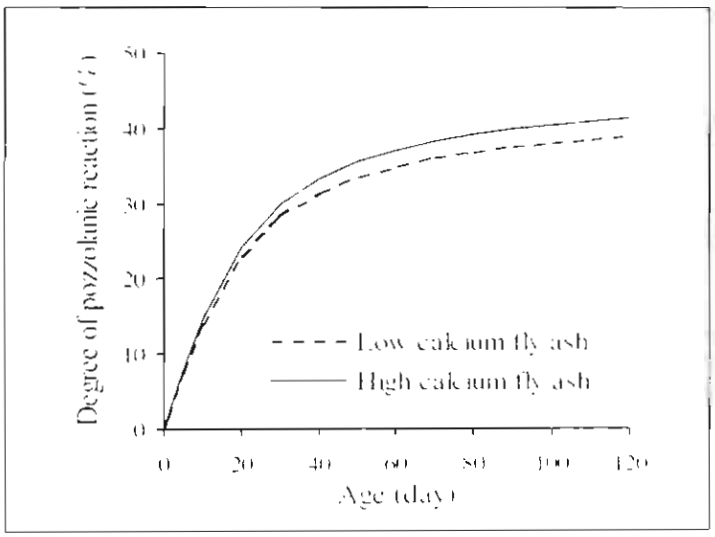

Fig. 2 Example of degree of pozzolanic reaction of fly ash (w/b=0.40, f/b=0.30)

3.2 Hydration products and pozzolanic products

It is assumed here for simplicity that the quantity of hydrated products of cement and pozzolanic products of fly ash are determined based on the reactions shown in Table 3. The quantity of products is calculated based on the reaction equations in that table and then corresponding hydrated mass of cement and reacted mass of fly ash.

Table 3 Reactions of cement and fly ash [16]

Materials	Reactions	Products
1. Cement		
C_3A	$2C_3A + 3C\underline{S}H_2 + 26H \longrightarrow C_6A\underline{S}_3H_{32}$	$C_6A\underline{S}_3H_{32}$
	$2C_3A + C_6A\underline{S}_3H_{32} + 4H \longrightarrow 3C_4A\underline{S}H_{12}$	$C_4A\underline{S}H_{12}$
	$C_3A + 6H \longrightarrow C_3AH_6$	C_3AH_6
C_4AF	$C_4AF + 3C\underline{S}H_2 + 21H \longrightarrow C_6A\underline{F}_2\underline{S}_3H_{32} + CAFH_2$	$C_6A\underline{F}_2\underline{S}_3H_{32}$
	$2C_4AF + C_6A\underline{F}_2\underline{S}_3H_{32} + 7H \longrightarrow C_4A\underline{F}\underline{S}H_{12} + 4CAFH_2$	$C_4A\underline{F}\underline{S}H_{12}$
	$C_4AF + 9H + 4CH \longrightarrow C_6AFH_{13}$	C_6AFH_{13}
C_3S	$2C_3S + 6H \longrightarrow C_3S_2H_3 + 3CH$	$C_3S_2H_3$
C_2S	$2C_2S + 4H \longrightarrow C_3S_2H_3 + CH$	$C_3S_2H_3$
2. Fly ash		
S	$2S + 3CH \longrightarrow C_3S_2H_3$	$C_3S_2H_3$
A	$2A + 3CH \longrightarrow C_3AH_6$	C_3AH_6

Notes: C = CaO, S = SiO_2, A = Al_2O_3, F = Fe_2O_3, H = H_2O, $\underline{S}$ = SO_3

3.3 Chemical binding

In general, a part of C_3A and C_4AF in cement firstly react with gypsum to form ettringite and monosulfate. Afterwards, the rest of unhydrated C_3A and C_4AF react further with water during curing period. It is considered that only some fractions of original content of C_3A and C_4AF are efficient for chemical binding. The efficient parts are those react during the chloride exposure period only and form Friedel's salt and calcium chloroferrite whereas those reacted before the chloride exposure period do not contribute to chemical binding. The fixed chloride content by chemical binding ($C_{fb,\ chem}(t, t_e)$) is defined as shown in Eq. 4. The time-dependent effects of curing time, t, and age at the end of chloride exposure, t_e, were taken into account in this equation.

$$C_{fb,\ chem}(t_s, t_e) = C_{fb,\ C_3A}(t_s, t_e) + C_{fb,\ C_4AF}(t_s, t_e) \quad (4)$$

where $C_{fb,\ C_3A}(t_s, t_e)$ and $C_{fb,\ C_4AF}(t_s, t_e)$ are the fixed chloride contents by chemical binding of C_3A and C_4AF, respectively during the exposure period of t_s-t_e.

The amount of $C_{fb,\ C_3A}(t_s, t_e)$ and $C_{fb,\ C_4AF}(t_s, t_e)$ can be determined from Eq. 5 and Eq. 6, respectively.

$$C_{fb,\ C_3A}(t_s, t_e) = \lambda_{fb,\ C_3A} \cdot (M_{n,\ C_3A}(t_e) - M_{n,\ C_3A}(t_s)) \quad (5)$$

$$C_{fb,\ C_4AF}(t_s, t_e) = \lambda_{fb,\ C_4AF} \cdot (M_{n,\ C_4AF}(t_e) - M_{n,\ C_4AF}(t_s)) \quad (6)$$

in which

$$\lambda_{fb,\ C_3A} = \frac{1.12}{3.3 - e^{(0.02 + \Delta\alpha_{C_3A})}} \quad (7)$$

and

$$\lambda_{fb,\ C_4AF} = \frac{0.6}{3.3 - e^{(0.02 + \Delta\alpha_{C_4AF})}} \quad (8)$$

where $\lambda_{fb,\ C_3A}$ and $\lambda_{fb,\ C_4AF}$ are defined as the fixed chloride ratios of C_3A and C_4AF, i.e., the ratios of fixed chloride to hydrated mass of C_3A and C_4AF, respectively, and $\Delta\alpha_{C_3A}$ and $\Delta\alpha_{C_4AF}$ are the changes of degree of hydration of C_3A and C_4AF, respectively during the exposure period.

The relationship between the fixed chloride ratios of C_3A and C_4AF and their respective changes of degree of hydration are shown in Fig. 3. The fixed chloride ratio decreases with the increase of the change of degree of hydration during the exposure period ($\Delta\alpha$) in Fig. 3. This implies that more chloride can chemically be bound at early hydrations of C_3A and C_4AF.

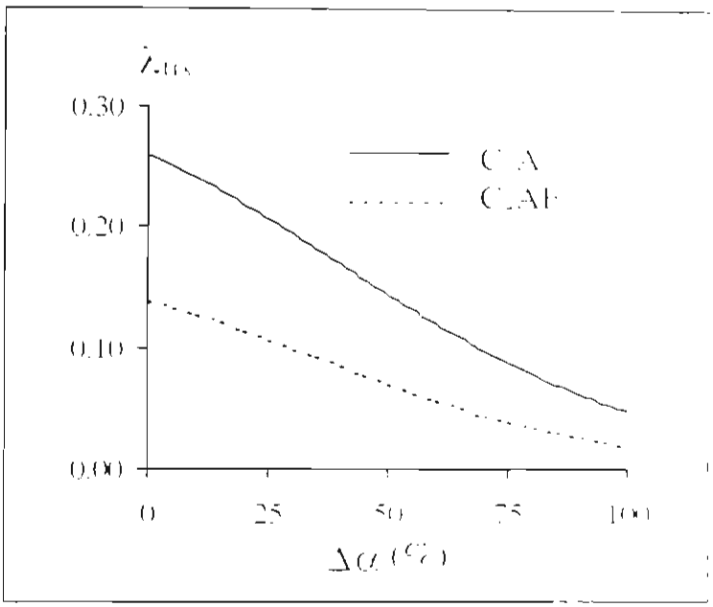

Fig. 3 Relationship between fixed chloride ratios of C_3A and C_4AF and change of degree of hydration during the exposure period

3.4 Physical binding

Chloride may be physically adsorbed on the surface of C-S-H gel and other products of reactions in cementitious system, such as C-A-H, C-A-F-H, ettringite and monosulfate. The fixed chloride content by physical binding at the end of chloride exposure ($C_{fix,phy}(t_e)$) is defined as in Eq. 9. This equation also takes into account the time-dependent effect of curing time plus chloride exposure period, t_e.

$$C_{fix,phy}(t_e) = \frac{\phi_{fix}}{100} \times \sum M_{product}(t_e) \qquad (9)$$

where ϕ_{fix} is the fixed chloride content of hydrated and pozzolanic products (%) and $\sum M_{product}(t_e)$ is the summation of mass of hydrated products and pozzolanic products at the end of chloride exposure.

For simplicity, it is assumed here that all hydrated and pozzolanic products have the same fixed chloride content. The fixed chloride content of hydrated and pozzolanic products depends on the total chloride content, water to binder ratio and fineness of cement in the cementitious system. The physically bound chloride content was derived from the back computation using test data of chloride binding capacity. The derived equation is shown in Eq. 10.

$$\phi_{fix} = \left(\frac{-0.093 \times w/b - 0.135}{0.037 + e^{(-0.0002 \cdot w/b^{-3.893} - 1.572 C_{tot})}} \right) \left(\frac{C_{tot}}{C_{tot} - 0.01} \right) \left(\frac{F_c}{3190} \right)^{1.5} \qquad (10)$$

where C_{tot} is the total chloride content (% by weight of binder), w/b is the water to binder ratio and F_c is the Blaine fineness of cement (cm^2/g).

As shown in Fig. 4, the physically bound chloride content of hydrated and pozzolanic products increases with increasing total chloride content and decreasing water to binder ratio.

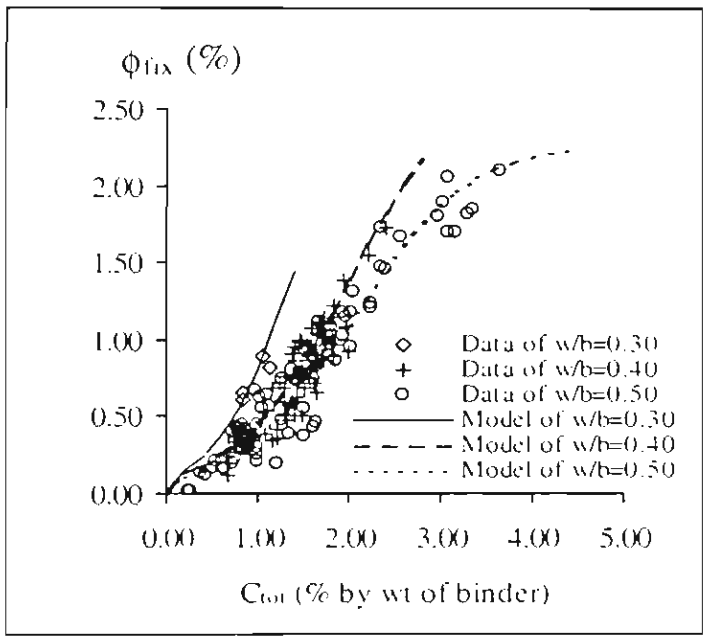

Fig. 4 Fixed chloride content for hydrated and pozzolanic products

4. RESULTS AND DISCUSSIONS

In this study, test of chloride binding capacity was conducted based on the fact that in most cases, chlorides attack concrete from outside environment. This type of chloride is called as external chloride in this paper. On the other hand, the chlorides present in concrete at start of concrete mixing is called as internal chloride. The test results of total chloride and fixed chloride are presented by bar charts. The values in parenthesis above the bar indicate the ratios of fixed chloride content to total chloride content.

It can be seen from Fig. 5 to Fig. 6 that the chloride binding capacity of cement paste exhibits a time dependent behavior. Considering samples with the same exposure period, t_e-t_s, paste with shorter curing time had higher total and fixed chloride content than that with longer one. The reason for larger total chloride content in shorter curing time case was that younger paste had bigger pore diameter, so larger amount of chloride can penetrate into the paste. Fixed chloride was also higher because there were larger amount of unhydrated aluminate and aluminoferrite phases, which were accessible for chloride binding. On the contrary, considering pastes with the same curing time, longer exposure period in saltwater resulted in higher total and fixed chloride content. Higher total chloride was just simply because of longer exposure period while the reason for larger fixed chloride content was that larger amount of hydrated and pozzolanic products produced during the longer exposure period can bind chlorides.

By comparing Fig. 5(a) with Fig. 5(b), it can be seen that at shorter exposure period, type III cement paste had higher fixed chloride content than type I cement paste. This was because type III cement had higher fineness than type I cement, so the hydration developed faster and higher hydration products was produced. This resulted in higher fixed chloride content. However, when exposure period was longer, the binding capacity of type I cement and type III cement was nearly the same.

When comparing Fig. 5(a) with Fig. 5(c), it can be observed clearly that type V cement paste had lower fixed chloride content than type I cement paste for all curing and exposure periods. This was mainly because the type V cement had lower content of C_3A than type I cement.

By considering the effect of water to cement ratio on chloride binding capacity in Fig. 6, it can be seen that when increasing water to cement ratio, though the total chloride content increased but the ratio of fixed chloride content to total chloride content decreased. This may be because chloride can be easier restrained, especially physically, in a denser paste.

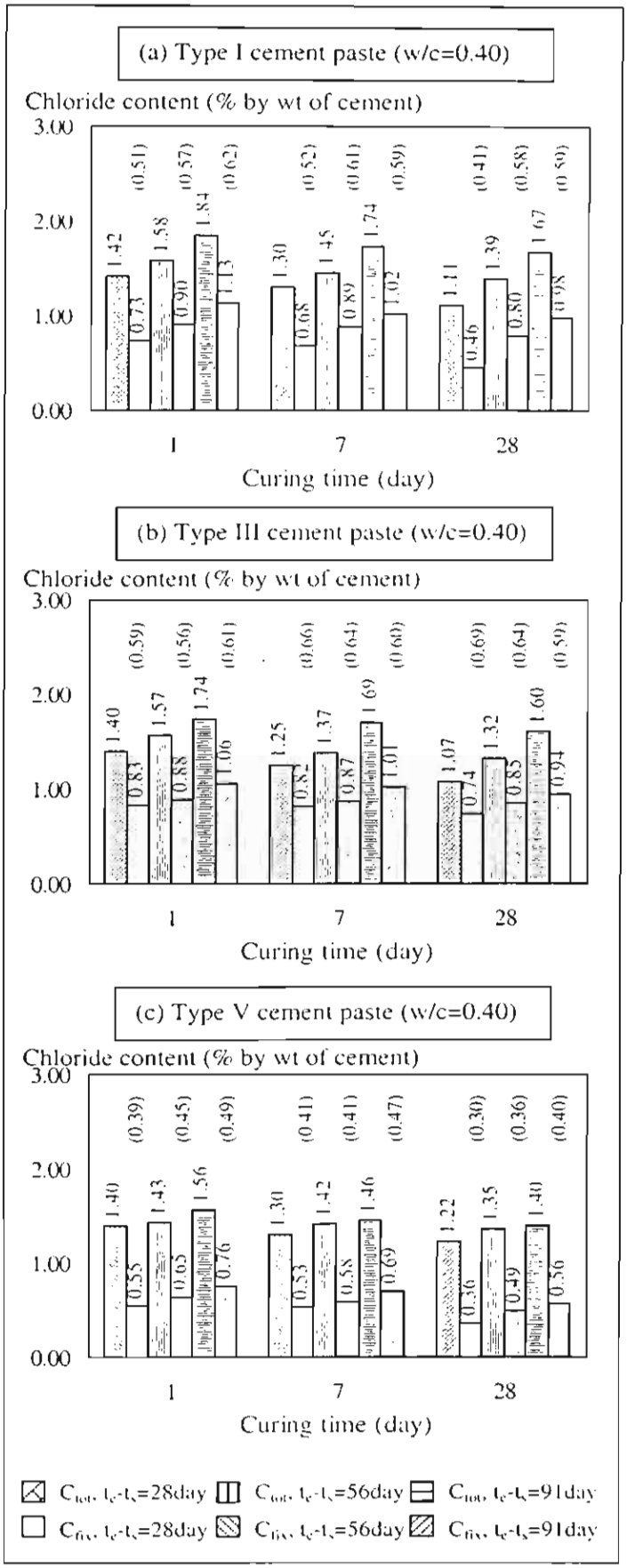

Fig. 5 Chloride binding capacity of various cement pastes

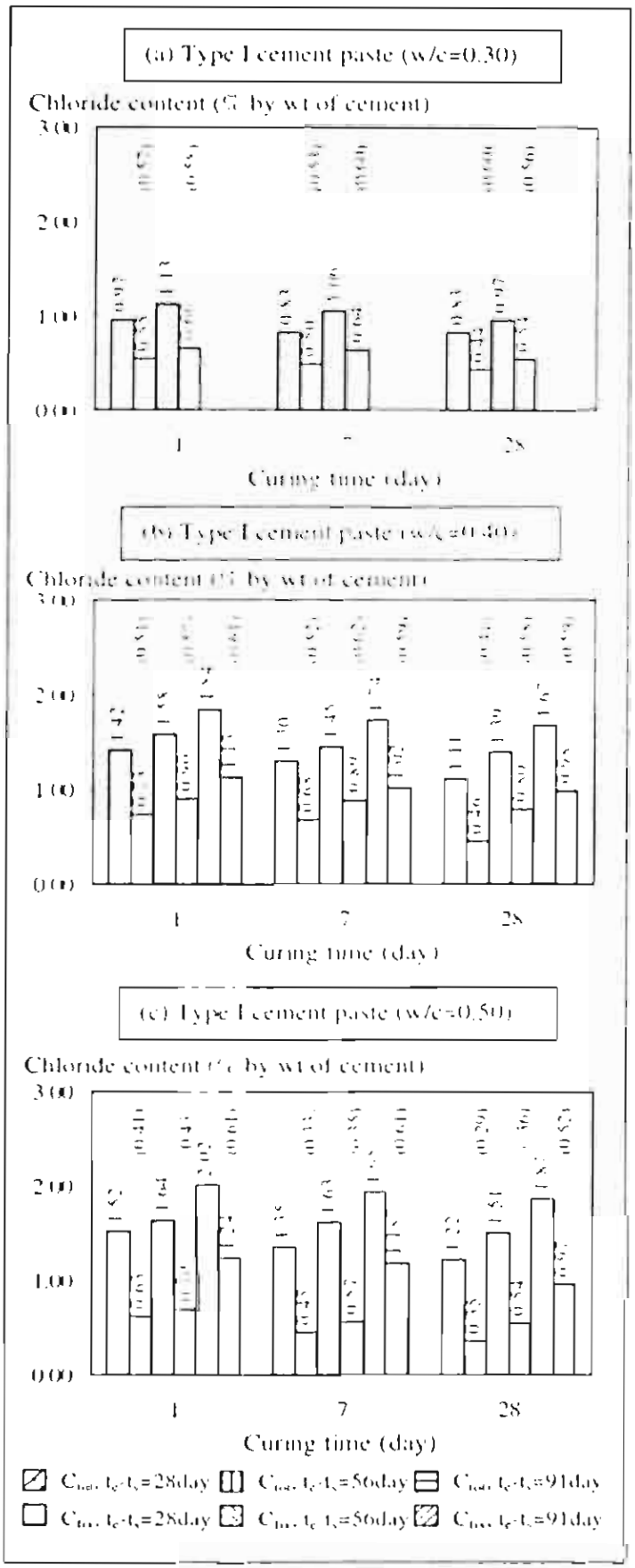

Fig. 6 Chloride binding capacity of cement paste with various water to cement ratios

In addition, Fig. 7 and Fig. 8 show that the characteristics of time-dependent chloride binding of cement-fly ash paste follow the same trend as those of the cement paste.

Fig. 7 and Fig. 8 illustrate that cement paste with high calcium fly ash had higher fixed chloride content than that with low calcium fly ash. This is because the high calcium fly ash usually contains some cementitious components which can hydrate to bind chloride and also to increase the early pozzolanic reaction so that higher pozzolanic products can be produced especially at the high replacement ratio.

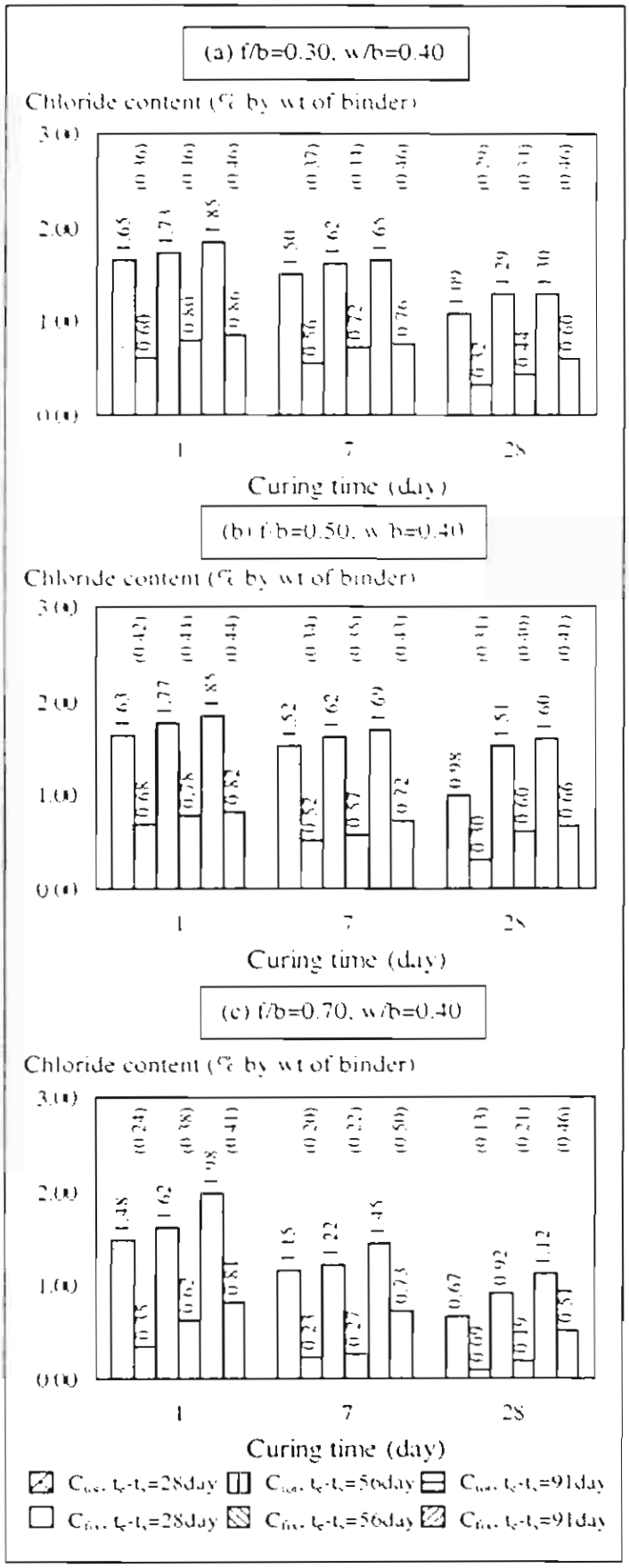

Fig. 7 Chloride binding capacity of type I cement – low calcium fly ash paste with various fly ash to binder ratios

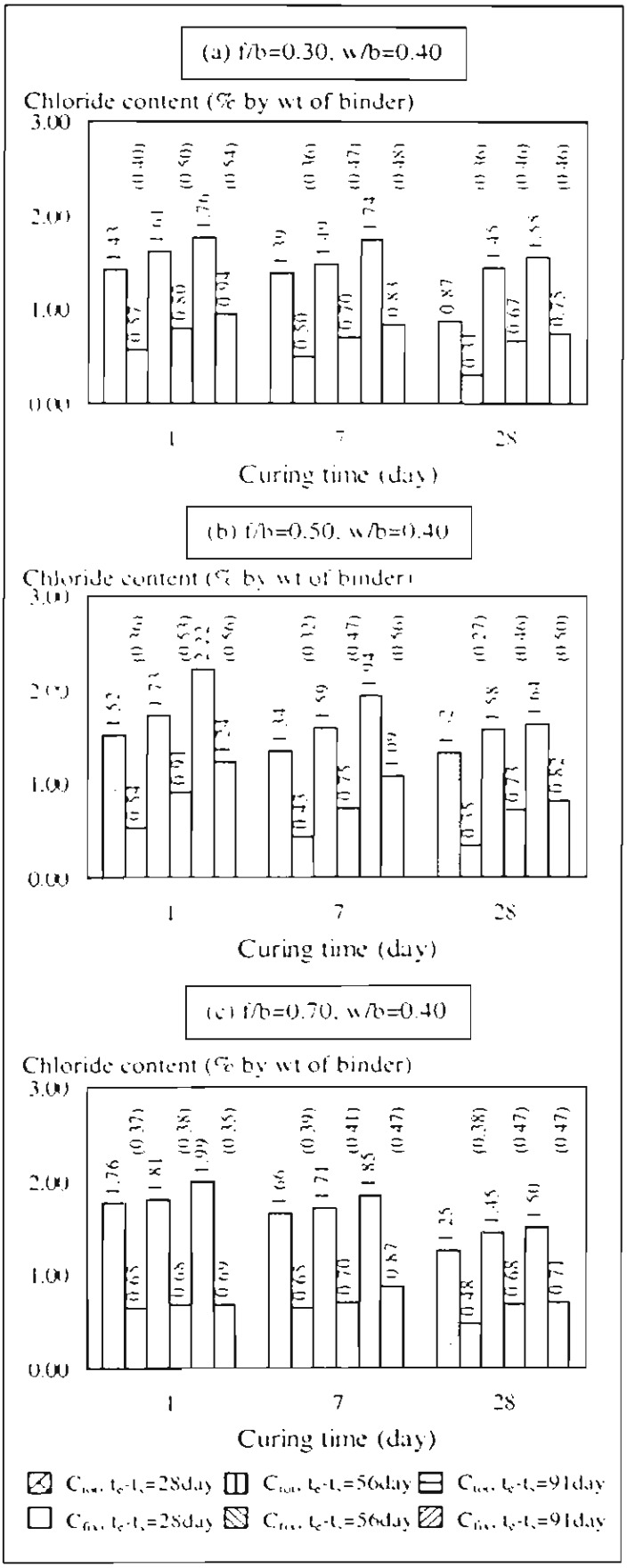

Fig. 8 Chloride binding capacity of type I cement – high calcium fly ash paste with various fly ash to binder ratios

5. VERIFICATIONS

The chloride binding capacity model was verified with test results obtained from both the authors and other researchers. The mix ingredients and chemical composition of materials from other researchers were briefly shown in Table 4. The verification was done on pastes, mortars and concretes with different types of cement and fly ash, fly ash replacement ratio, water to binder ratio, curing time and chloride exposure period.

Table 4 Mixture conditions and properties of materials from other researchers

Researchers	Rasheeduzzafar [4]				Hussain [8]			Arya [1]	Maruya [17]	
Specimen type	cement paste				cement paste			cement paste	Cement mortar, fly ash mortar and concrete	
w/b	0.60				0.60			0.50	0.50	
f/b	0				0			0	0.30	
Chloride type	internal				internal			external	external	
Chloride content	0.50%, 0.98%, 1.20% by wt of cement				0.60%, 1.20% by wt of cement			12.1 g/l	18.2 g/l	
Materials	C	C	C	C	C	C	C	C	C	FA
Curing time (day)	0	0	0	0	0	0	0	2, 28, 84	28	
Chloride exposure period (day)	180	90	90	180	180	180	180	28, 56, 84	28, 91, 182, 365	
Chemical compositions										
SiO_2 (%)	21.90	20.76	20.90	19.92	21.90	20.90	19.92	19.60	20.50	55.00
Al_2O_3 (%)	3.95	4.73	5.00	6.54	3.95	5.26	6.54	5.10	5.00	5.60
Fe_2O_3 (%)	4.80	2.40	3.05	2.09	4.80	3.75	2.09	3.10	3.00	2.20
CaO (%)	64.20	63.92	64.50	64.70	64.20	65.03	64.70	65.20	63.40	6.90
SO_3 (%)	1.71	3.00	3.21	2.61	1.71*	2.54*	2.61*	3.00	2.00	0.50
Loss on ignition (%)	1.10	0.71	2.15	1.10	1.10	-	1.10	1.50	1.80	1.00
Bogue's potential compound compositions										
C_3S (%)	54.30	57.17	57.80	54.50	54.30	55.83	54.50	55.20	58.60	
C_2S (%)	21.80	16.53	16.50	16.00	21.80	17.80	16.00	14.80	14.60	
C_3A (%)	2.43	7.37	9.10	14.00	2.43	7.59	14.00	9.90	8.20	
C_4AF (%)	14.61	9.27	7.40	6.50	14.61	11.41	6.50	9.70	9.10	

Notes: C = Cement, FA = Fly ash

* SO_3 contents were also raised to 4.00% and 8.00% by adding sodium sulfate into the pastes

Fig. 9 and Fig. 10 show the verification of model with the experimental results conducted by the authors. In each figure, the fixed chloride contents calculated from model are compared with that from experiment. It can be seen from the figures that the model can be used to predict the chloride binding capacity of cement pastes and cement fly-ash pastes at various curing time and chloride exposure period up to a certain satisfactory degree.

Fig. 11 to Fig. 14 demonstrate the verification of the model with the test results from other researchers. Fig. 11 and Fig. 12 show the verification of model with results from internal chloride test, while Fig. 13 and Fig. 14 show the verification of model with results from external chloride test.

As indicated in Fig. 11 and Fig. 12, the model can be used to predict the chloride binding capacity of cement pastes with various C_3A contents from 2.43% to 14.00% and SO_3 contents from 1.7% to 8.0%.

As illustrated in Fig. 13 and Fig. 14, the model can also be applied to predict the chloride binding capacity of various cement pastes, mortars, fly-ash mortars and concretes.

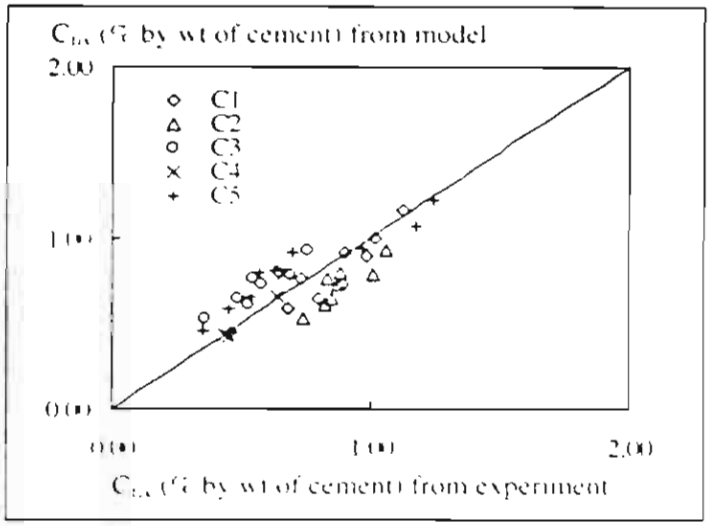

Fig. 9 Verification of model with various cement pastes in this study

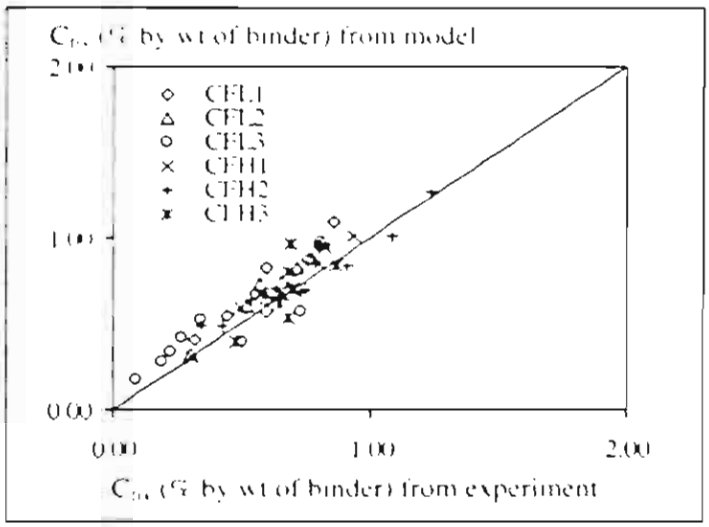

Fig. 10 Verification of model with various cement-fly ash pastes in this study

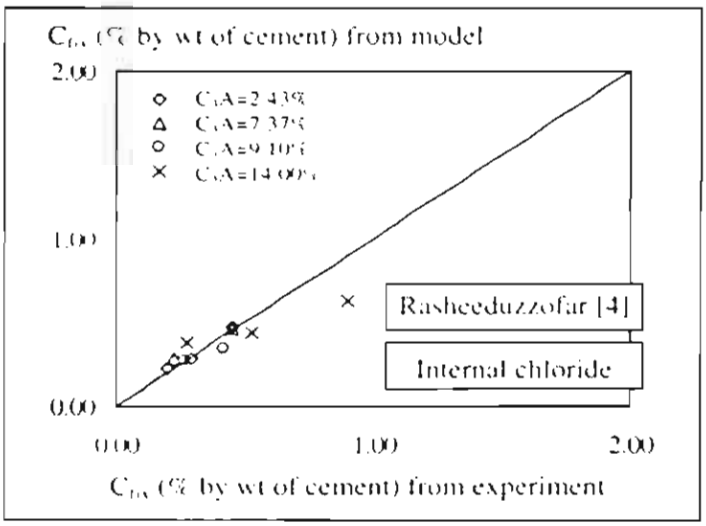

Fig. 11 Verification of model for various C_3A content of cement paste

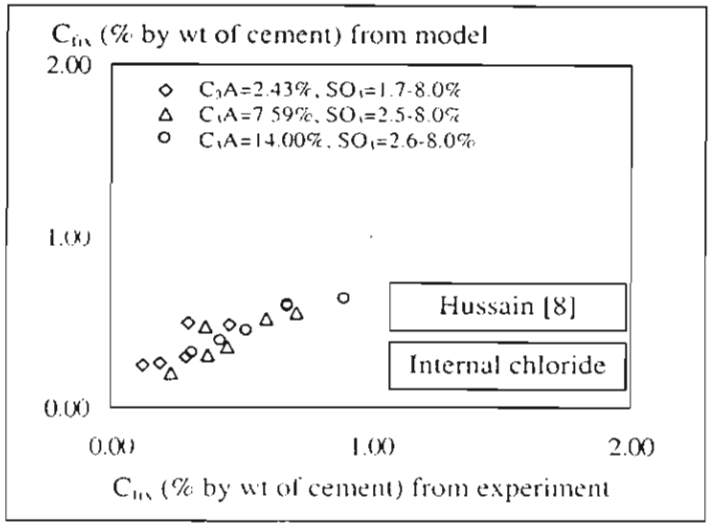

Fig. 12 Verification of model for various C_3A and SO_3 content of cement

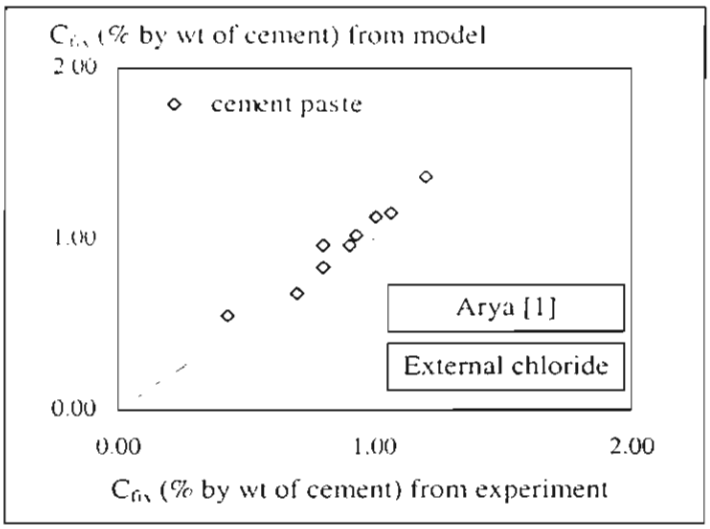

Fig. 13 Verification of model for cement paste

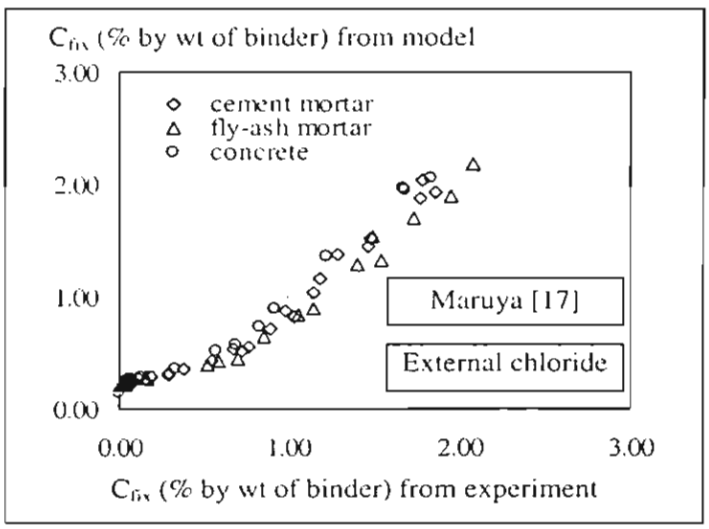

Fig. 14 Verification of model for cement mortar, fly-ash mortar and concrete

6. CONCLUSIONS

Based on the experimental results, the model formation and the verification of model, the following conclusions can be drawn.

1. The behavior of chloride binding capacity of cement-fly ash cementitious system was time-dependent. Chloride binding depended on the curing and chloride exposure periods. Pastes having older age prior to chloride attack bound less amount of chloride than those exposed to chloride at younger age. Longer exposure period of paste resulted in larger chloride binding capacity.
2. Cement pastes with high calcium fly ash had higher fixed chloride content than those with low calcium fly ash. This is because the high calcium fly ash usually contains some cementitious components which can hydrate to bind chloride and also to increase the early pozzolanic reaction so that higher pozzolanic products can be produced especially at the high replacement ratio
3. A model for predicting chloride binding capacity of cement-fly ash cementitious system was proposed by considering that the unhydrated aluminate (C_3A) and aluminoferrite (C_4AF) phases in cement were considered responsible for the chemical binding, while the hydrated products from cement and pozzolanic products from fly ash were responsible for physical binding.
4. The proposed model can satisfactorily predict the chloride binding capacity of various cement pastes and cement-fly ash pastes with different mixture proportion, properties of cement and fly ash, curing time and chloride exposure period.

ACKNOWLEDGMENTS

The authors gratefully acknowledge the support provided for this research by the Thailand Research Fund (TRF).

REFERENCES

[1] Arya C., Buenfeld N.R., Newman J.B., 'Factors influencing chloride-binding in concrete', *Cement and Concrete Research* **20** (1990) 291-300

[2] Ramachadran S., Seeley R.C., Polomark G.M., 'Free and combined chloride in hydrating cement and cement compounds', *Materials and Structures* **17** (1984) 285-289

[3] Theissing E.M., Mebius-Van De Laar T., De Wind G., 'The combining of sodium chloride and calcium chloride by the hardened Portland cement compounds C_3S, C_2S, C_3A and C_4AF', (Proceedings of 8th International Symposium on Chemistry of Cement, Rio de Janeiro, 1986, 823-828)

[4] Rasheeduzzafar, Hussain E.S., Al-Saadoun S.S., 'Effect of cement composition on chloride binding and corrosion of reinforcing steel in concrete', *Cement and Concrete Research* **21** (1991) 777-794

[5] Suryavanshi A.K., Scantlebury J.D., Lyon S.B., 'The binding of chloride ions by sulphate resistant Portland cement', *Cement and Concrete Research* **25** (1995) 581-592

[6] Csizmadia J., Balazs G., Tamas F.D., 'Chloride ion binding capacity of aluminoferrites', *Cement and Concrete Research* **31** (2001) 577-588

[7] Dhir R.K., El-Mohr M.A.K., Dyer T.D., 'Chloride Binding in GGBS concrete', *Cement and Concrete Research* **26** (1996) 1767-1773

[8] Hussain E.S., Rasheeduzzafar, Al-Gahtani A.S., 'Influence of sulfates on chloride binding in cements', *Cement and Concrete Research* **24** (1994) 8-24

[9] Xu Y., 'The influence of sulphates on chloride binding and pore solution chemistry', *Cement and Concrete Research* **27** (1997) 1841-1850

[10] Jensen O.M.., Korzen M.S.H., Jakobsen H.J., Skibsted J., 'Influence of cement constitution and temperature on chloride binding in cement paste', *Advances in Cement Research* **12** (2000) 57-64
[11] Luping T., Nilsson L.-O., 'Chloride binding capacity and binding isotherms of OPC pastes and mortars', *Cement and Concrete Research* **23** (1993) 247-253
[12] Delagrave A., Marchand J., Ollivier J.P., Julien S., Hazrati K., 'Chloride binding capacity of various hydrated cement paste systems', *Advanced Cement Based Materials* **6** (1997) 28-35
[13] Jensen H.-U., Pratt P.L., 'The binding of chloride ions by pozzolanic product in fly ash cement blends', *Advances in Cement Research* **2** (1989) 121-129
[14] Nipatsat, N., Tangtermsirikul S., 'Compressive strength prediction model for fly ash concrete', *Thammasat International Journal of Science and Technology* **11** (2000) 1-7
[15] Tangtermsirikul S., Tatong, S., 'Modeling of aggregate stiffness and its effects on shrinkage of concrete', *Science Asia* **27** (2001) 185-192
[16] Mindess S., Young J.F., 'Concrete', (Prentice-Hall, New Jersey, 1981)
[17] Maruya T., 'Simulation of chloride ion movement in hardened concrete', A Ph.D dissertation, department of civil engineering, University of Tokyo, Japan, 1995 (in Japanese)

3. ผลงานตีพิมพ์ในวารสารวิชาการในประเทศและการนำเสนอผลงานในที่ประชุมวิชาการ

3.1 T. Sumranwanich and S. Tangtermsirikul, A chloride binding capacity model for cement-fly ash pastes, 27th Conference on Our World in Concrete & Structures, Singapore, August 29-30, 2002, pp. 545-552

A chloride binding capacity model for cement-fly ash pastes

T Sumranwanich [illegible]
S Tangtermsirikul [illegible]

Abstract

A chloride binding capacity model for cement-fly ash pastes taking into account both chemical binding and physical binding was proposed. Chemical binding depended on the amount of unhydrated aluminate and aluminoferrite phases while physical binding depended upon the quantity of hydrated and pozzolanic products. The chloride binding of cement paste and cement-fly ash pastes under different curing time and chloride exposure period were investigated. The experimental results showed a time-dependent behavior of chloride binding capacity. At the same chloride exposure period, pastes with longer curing time prior to chloride exposure bound less amount of chloride than those exposed with shorter curing time. Longer exposure period of paste resulted in larger content of bound chloride. The analytical results from model were verified with the experimental results and the verification showed that the proposed model was satisfactory for predicting the chloride binding capacity of cement and cement-fly ash pastes.

Keywords: chloride, chloride binding, corrosion, cement paste, fly ash

1. Introduction

The ability of hydrating cement to bind chlorides from the pore solution in concrete is one of the important factors which controls corrosion of steel. This is because only free chlorides present in the pore solution can initiate the corrosion. Therefore, chloride binding capacity is a significant property of concrete for prolonging the service life of the reinforced concrete structures under chloride environment. There are many factors that govern the chloride binding capacity, such as cement type, fly ash type, curing time prior to chloride attack, exposure period with chloride and so on.

Chloride binding capacity of various cementitious pastes had been studied by many researchers [1-3]. Some proposed a model for predicting the chloride binding capacity of cement-ground granulated blastfurnace slag paste [3]. However, there is still no any model that considers the effect of curing time and chloride exposure period in the prediction of chloride binding capacity of cement-fly ash paste. The time-dependent chloride binding capacity of paste depended on age of paste at start of chloride exposure and the chloride exposure period.

The aim of this study is to propose a model for predicting chloride binding capacity of cement-fly ash pastes based on mixture proportion and properties of cementitious materials. The time-dependent effects of curing time prior to chloride attack and chloride exposure period on the chloride binding capacity were considered in the model. Both chemical binding and physical binding were included into the model. The validity of the model was verified by the experimental results.

2. Experimental Program

2.1 Materials, mix proportion and specimen preparation

Type I Portland cement has been used in this study. Two types of fly ash corresponding to ASTM F-type (low calcium fly ash) and ASTM C-type (high calcium fly ash) were mixed with type I Portland cement for producing the cement-fly ash pastes. The chemical composition and physical properties of cement and fly ash are listed in Table 1.

Table 1 Chemical compositions and physical properties of Portland cement and fly ash

Chemical compositions	Type I Portland cement	Low calcium fly ash (F-type)	High calcium fly ash (C-type)
SiO_2 (%)	20.61	45.88	38.42
Al_2O_3 (%)	5.03	26.20	19.17
Fe_2O_3 (%)	3.03	10.94	10.93
CaO (%)	64.89	8.28	17.28
MgO (%)	1.43	2.83	7.95
SO_3 (%)	2.70	1.04	2.01
Na_2O (%)	0.22	0.90	1.03
K_2O (%)	0.46	2.78	2.28
Free lime (%)	0.79	-	-
Loss on ignition (%)	1.23	0.17	0.05
Physical properties			
Blaine fineness (cm^2/g)	3,190	3,460	3,510
Specific gravity	3.15	2.03	2.10

Seven different mixture conditions of cementitious paste were prepared for this investigation, as shown in Table 2. There were one mixture condition of cement paste and six mixture conditions of cement-fly ash paste.

In order to achieve rapid saturation, thin disc specimens of 50 mm diameter and 10 mm thick cast in PVC molds were selected for sample preparation. Thirteen specimens were prepared for each mixture condition, ten for expressing the pore solution and three for determining the evaporable water content. The mixing procedure was performed according to ASTM C305.

2.2 Curing time and chloride exposure period

After casting, specimens were sealed with plastic sheet to prevent drying for 24 hours. Except for specimens to be exposed to chloride at 1 day, all specimens were cured in water immediately after removal from the molds. Curing times were 1, 7 and 28 days as shown in Table 2. The curing temperature was 30±2°C.

Table 2 Mixture conditions

Mix Designation	Materials		w/b	f/b	Curing time (day)	Chloride exposure period (day)
	Cement type	Fly ash type				
C1	Type I	-	0.40	0	1, 7, 28	28, 56, 91
CFL1	Type I	F*	0.40	0.30	1, 7, 28	28, 56, 91
CFL2	Type I	F*	0.40	0.50	1, 7, 28	28, 56, 91
CFL3	Type I	F*	0.40	0.70	1, 7, 28	28, 56, 91
CFH1	Type I	C**	0.40	0.30	1, 7, 28	28, 56, 91
CFH2	Type I	C**	0.40	0.50	1, 7, 28	28, 56, 91
CFH3	Type I	C**	0.40	0.70	1, 7, 28	28, 56, 91

* F-type fly ash has (SiO_2 + Al_2O_3 + Fe_2O_3) content greater than 70%, but low in CaO content. It is called *low calcium fly ash* in this study.

** C-type fly ash has (SiO_2 + Al_2O_3 + Fe_2O_3) content less than 70%, but larger in CaO content. It is called *high calcium fly ash* in this study.

At the end of water curing, specimens were exposed to chloride by submerging in salt water with 3.0 % of chloride ion concentration (30 gram per liter) for different exposure periods. The exposure periods were 28, 56 and 91 days as shown in Table 2. The volume of salt water (chloride solution) was 2.0 liters. The temperature during the chloride exposure period was 30±2°C.

2.3 Determination of chloride content

At the end of chloride exposure period, specimens were removed from salt water. Surfaces of specimen were dried by using tissue paper. Pore solution inside the specimens was obtained by using a pore expressing apparatus. The maximum loading pressure for expressing the pore solution was about 500 MPa. Two or three cycles of loading and unloading were performed in order to get 3 to 5 cm^3 of pore solution. The evaporable water content of specimen was immediately tested for being used in the determination of free chloride in the specimen.

Total chloride was determined from the difference between initial chloride content of the submerging salt water at the start of exposure and its final chloride content at the end of exposure and shared equally to all specimens submerged in the salt water. The free chloride was determined from chloride concentration of pore solution expressed from specimen multiplied with the evaporable water. Finally, the fixed chloride of cementitious paste can be determined by subtracting the total chloride with the free chloride. All chloride concentrations were analyzed by potentiometric titration with $AgNO_3$ solution and chloride ion selective electrode.

3. Model of Time-Dependent Chloride Binding Capacity

The chloride binding capacity model of cement-fly ash paste considers both chemical binding and physical binding as given in Eq. 1. The aluminate phase, C_3A, and aluminoferrite phase, C_4AF, in cement were considered responsible for the chemical binding while the hydrated products from cement and pozzolanic products from fly ash, such as C-S-H, C-A-H, C-A-F-H, ettringite and monosulfate were responsible for physical binding.

$$C_{fix}(t_s, t_e) = C_{fix,chem}(t_s, t_e) + C_{fix,phy}(t_e) \quad (1)$$

where C_{fix} (t_s, t_e) is the total fixed chloride content in the cementitious system (% by weight of binder), $C_{fix,\ chem}$ (t_s, t_e) is the fixed chloride content by chemical binding (% by weight of binder), $C_{fix,\ phy}$ (t_e) is the fixed chloride content by physical binding (% by weight of binder), t_s is the age at the start of chloride exposure which is equal to curing time and t_e is the age at the end of chloride exposure. It is noted that t_e- t_s means the chloride exposure period.

3.1 Hydrated mass of cement and reacted mass of fly ash

3.1.1 Hydrated mass of cement

The mass of each major compound in Portland cement was calculated based upon Bogue's equation. The hydrated mass of compound i at age t was determined from Eq. 2.

$$M_{hyd,i}(t) = M_i \times \frac{\alpha_i(t)}{100} \quad , i = C_3A,\ C_4AF,\ C_3S,\ C_2S \quad (2)$$

where $M_{hyd,\ i}(t)$ is the hydrated mass of compound i at age t days (kg/m^3 of concrete), M_i is the mass of each major compound in Portland cement (kg/m^3 of concrete), $\alpha_i(t)$ is the degree of hydration of compound i of cement at age t days (%) and t is the age of the sample (day). It is noted that the age is equal to zero at start adding water to the mixture.

The details of degree of hydration of each oxide compound are not provided in this paper but elsewhere [4] since they are not the direct scope of this study. However, the degree of hydration of each major compound of cement in the paste with w/c of 0.40 is shown in Fig. 1.

3.1.2 Reacted mass of fly ash

The reacted mass of fly ash in the pozzolanic reaction at age t days was calculated according to Eq. 3.

$$M_{poz,fa}(t) = M_{fa} \times \frac{\alpha_{fa}(t)}{100} \quad (3)$$

where $M_{poz,\ fa}(t)$ is the reacted mass of fly ash at age t days (kg/m^3 of concrete), M_{fa} is the mass of fly ash (kg/m^3 of concrete) and $\alpha_{fa}(t)$ is degree of pozzolanic reaction of fly ash at age t days (%).

The degree of pozzolanic reaction of low and high calcium fly ashes in the pastes with w/b of 0.40 and f/b of 0.30, 0.50 and 0.70 used in this model are shown in Fig. 2 [5].

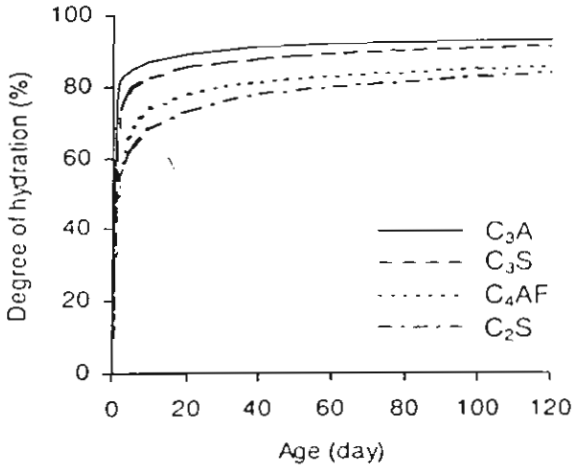

Fig. 1 Example of degree hydration of type I cement (w/c=0.40)

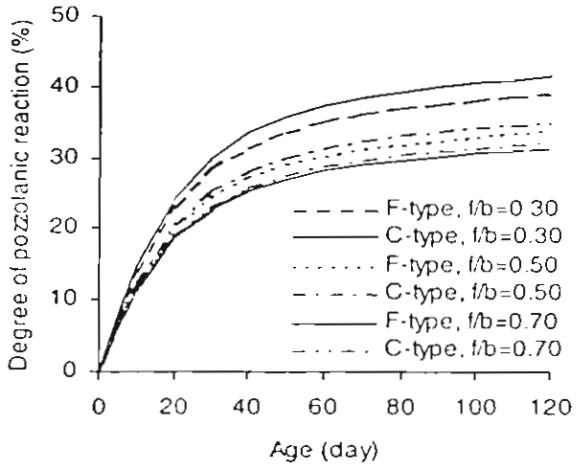

Fig. 2 Example of degree of pozzolanic reaction of fly ash (w/b=0.40, f/b=0.30)

3.2 Hydration products and pozzolanic products

It is assumed here for simplicity that the quantity of hydrated products of cement and pozzolanic products of fly ash are determined based on the reactions shown in Table 3. The quantity of products is calculated based on the reaction equations in that table and their corresponding hydrated mass of cement and reacted mass of fly ash.

Table 3 Reactions of cement and fly ash

Materials	Reactions	Products
1. Cement		
C_3A	$2C_3A + 3C\underline{S}H_2 + 26H \longrightarrow C_6A\underline{S}_3H_{32}$ $2C_3A + C_6A\underline{S}_3H_{32} + 4H \longrightarrow 3C_4A\underline{S}H_{12}$ $C_3A + 6H \longrightarrow C_3AH_6$	$C_6A\underline{S}_3H_{32}$ $C_4A\underline{S}H_{12}$ C_3AH_6
C_4AF	$C_4AF + 3C\underline{S}H_2 + 21H \longrightarrow C_6(A,F)\underline{S}_3H_{32} + (A,F)H_3$ $2C_4AF + C_6(A,F)\underline{S}_3H_{32} + 7H \longrightarrow C_4(A,F)\underline{S}H_{12} + (A,F)H_3$ $C_4AF + 9H + 4CH \longrightarrow C_4(A,F)H_{13}$	$C_6(A,F)\underline{S}_3H_{32}$ $C_4(A,F)\underline{S}H_{12}$ $C_4(A,F)H_{13}$
C_3S	$2C_3S + 6H \longrightarrow C_3S_2H_3 + 3CH$	$C_3S_2H_3$
C_2S	$2C_2S + 4H \longrightarrow C_3S_2H_3 + CH$	$C_3S_2H_3$
2. Fly ash		
S	$2S + 3CH \longrightarrow C_3S_2H_3$	$C_3S_2H_3$
A	$2A + 3CH \longrightarrow C_3A_2H_3$	$C_3A_2H_3$

Notes: C = CaO, S = SiO_2, A = Al_2O_3, F = Fe_2O_3, H = H_2O, $\underline{S}$ = SO_3

3.3 Chemical binding

In general, a part of C_3A and C_4AF in cement firstly react with gypsum to form ettringite and monosulfate. Afterwards, the rest of unhydrated C_3A and C_4AF hydrate further during curing period. It is considered that only some fractions of original content of C_3A and C_4AF are efficient for chemical binding. The efficient parts are those react during the chloride exposure period only and form Friedel's salt and calcium chloroferrite whereas those reacted before the chloride exposure period do not contribute to chemical binding. The fixed chloride content by chemical binding ($C_{fix,\,chem}(t_s,\,t_e)$) is defined as shown in Eq. 4. The time-dependent effects of curing time, t_s, and age at the end of chloride exposure, t_e, were taken into account in this equation.

$$C_{fix,chem}(t_s,t_e) = C_{fix,C_3A}(t_s,t_e) + C_{fix,C_4AF}(t_s,t_e) \quad (4)$$

where $C_{fix,\,C3A}(t_s,\,t_e)$ and $C_{fix,\,C4AF}(t_s,\,t_e)$ are the fixed chloride contents by chemical binding of C_3A and C_4AF, respectively during the exposure period of t_e-t_s.

The amount of $C_{fix,\,C3A}(t_s,\,t_e)$ and $C_{fix,\,C4AF}(t_s,\,t_e)$ can be determined from Eq. 5 and Eq. 6, respectively.

$$C_{fix,C3A}(t_s,t_e) = \lambda_{fix,C_3A} \times \left(M_{hyd,\,C_3A}(t_e) - M_{hyd,\,C_3A}(t_s)\right) \quad (5)$$

$$C_{fix,C4AF}(t_s,t_e) = \lambda_{fix,C_4AF} \times \left(M_{hyd,\,C_4AF}(t_e) - M_{hyd,\,C_4AF}(t_s)\right) \quad (6)$$

in which

$$\lambda_{fix,C3A} = \frac{1.12}{3.3 + e^{(0.03 \times \Delta\alpha_{C3A})}} \quad (7)$$

and

$$\lambda_{fix,C4AF} = \frac{0.6}{3.3 + e^{(0.033 \times \Delta\alpha_{C4AF})}} \quad (8)$$

where $\lambda_{fix,\ C3A}$ and $\lambda_{fix,\ C4AF}$ are defined as the fixed chloride ratios of C_3A and C_4AF, i.e., the ratios of fixed chloride to hydrated mass of C_3A and C_4AF, respectively, and $\Delta\alpha_{C3A}$ and $\Delta\alpha_{C4AF}$ are the changes of degree of hydration of C_3A and C_4AF, respectively during the exposure period.

The relationship between the fixed chloride ratios of C_3A and C_4AF and their respective changes of degree of hydration are shown in Fig. 3. The fixed chloride ratio decreases with the increase of the change of degree of hydration during the exposure period ($\Delta\alpha$ in Fig. 3). This implies that more chloride can chemically be bound at early hydrations of C_3A and C_4AF than that at the later hydrations

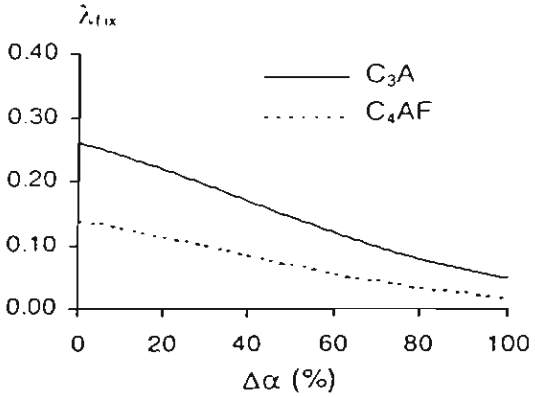

Fig. 3 Relationship between fixed chloride ratios of C_3A and C_4AF and change of degree of hydration of C_3A and C_4AF during the exposure period

3.4 Physical binding

Chloride may be physically adsorbed on the surface of C-S-H gel and other products of reactions in cementitious system, such as C-A-H, C-A-F-H, ettringite and monosulfate. The fixed chloride content by physical binding at the end of chloride exposure ($C_{fix,\ phy}(t_e)$) is defined as in Eq. 9. This equation also takes into account the time-dependent effect of curing time plus chloride exposure period, t_e.

$$C_{fix,phy}(t_e) = \frac{\phi_{fix}}{100} \times \sum M_{product}(t_e) \quad (9)$$

where ϕ_{fix} is the fixed chloride content of hydrated and pozzolanic products (%) and $\Sigma M_{\ product}(t_e)$ is the summation of mass of hydrated products and pozzolanic products at the end of chloride exposure.

For simplicity, it is assumed here that all hydrated and pozzolanic products have the same fixed chloride content. The fixed chloride content of hydrated and pozzolanic products depends on the total chloride content, water to binder ratio and fineness of cement in the cementitious system. The physically bound chloride content was derived from the back computation using test data of chloride binding capacity. The derived equation is shown in Eq. 10 (See Fig. 4).

$$\phi_{fix} = \left(\frac{-0.093 \times w/b + 0.135}{0.037 + e^{\left(-0.0002 \times w/b^{(-6.593)} - 1.572\right) C_{tot}}} \right) \left(\frac{C_{tot}}{C_{tot} + 0.01} \right) \left(\frac{F_C}{3190} \right)^{0.5} \quad (10)$$

where C_{tot} is the total chloride content (% by weight of binder), w/b is the water to binder ratio and F_c is the Blaine fineness of cement (cm^2/g)

As shown in Fig. 4, the physically bound chloride content of hydrated and pozzolanic products increases with increasing total chloride content and decreasing water to binder ratio.

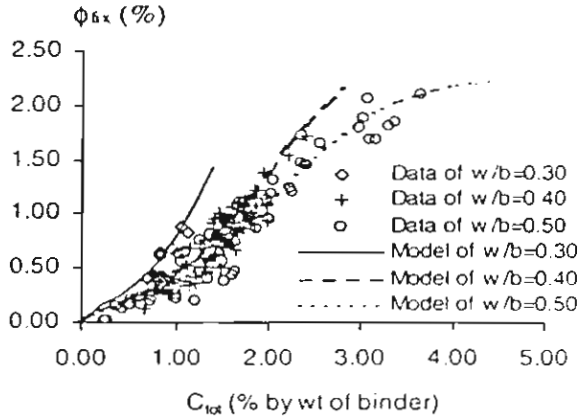

Fig. 4 Fixed chloride content for hydrated and pozzolanic products

4. Results and Discussions

The test results of total chloride and fixed chloride are presented by bar charts. The values in parenthesis above the bar indicate the ratios of fixed chloride content to total chloride content.

It can be seen from Fig. 5 that the chloride binding capacity of cement paste exhibits a time dependent behavior. Considering samples with the same exposure period, t_e-t_s, paste with shorter curing time had higher total and fixed chloride content than that with longer one. The reason for larger total chloride content in shorter curing time case was that younger paste was more porous, so larger amount of chloride could penetrate into the paste. Fixed chloride was also higher because there were larger amount of unhydrated aluminate and aluminoferrite phases, which were accessible for chloride binding. On the contrary, considering pastes with the same curing time, longer exposure period in saltwater resulted in higher total and fixed chloride content. Higher total chloride was just simply because of longer exposure period while the reason for larger fixed chloride content was that larger amount of hydrated and pozzolanic products produced during the longer exposure period can bind chlorides.

In addition, Fig. 6 and Fig. 7 show that the characteristics of time-dependent chloride binding of cement-fly ash paste follow the same trend as that of the cement paste. Furthermore, cement paste with high calcium fly ash had higher fixed chloride content than that with low calcium fly ash. This is because high calcium fly ash usually contains some cementitious components which can hydrate to bind chloride and also to increase the early pozzolanic reaction so that higher products from fly ash reactions can be produced especially at the high replacement ratio.

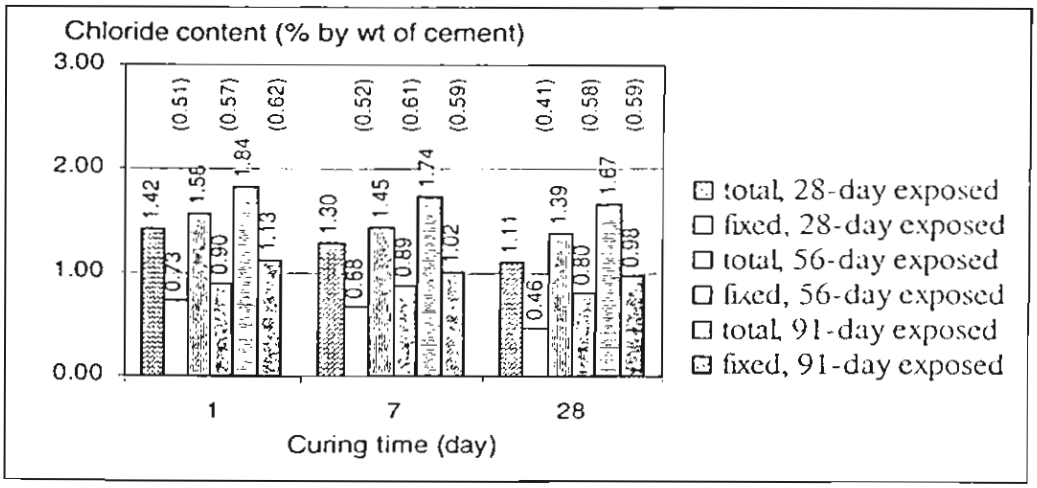

Fig. 5 Chloride binding capacity of type I cement paste

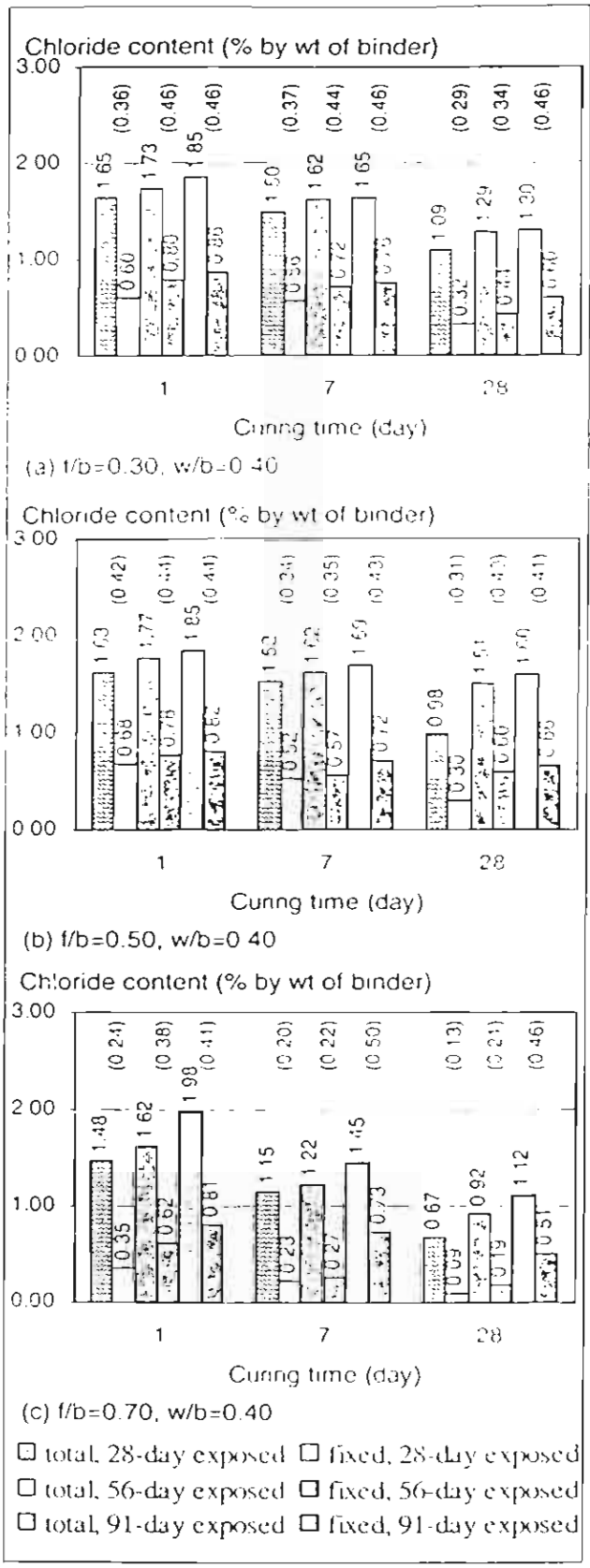

Fig. 6 Chloride binding capacity of type I cement – low calcium fly ash paste with various fly ash to binder ratios

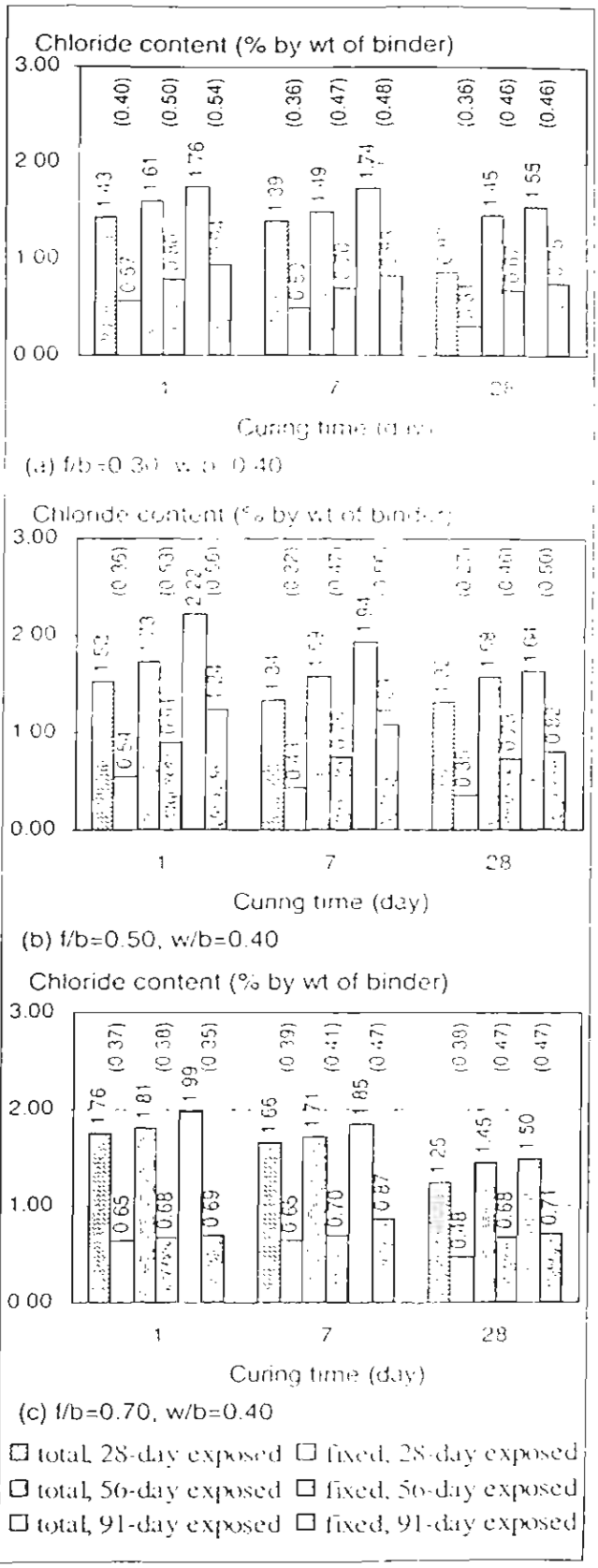

Fig. 7 Chloride binding capacity of type I cement – high calcium fly ash paste with various fly ash to binder ratios

5. Verifications

The chloride binding capacity model was verified with test results as shown in Fig. 8 and Fig. 9. In each figure, the fixed chloride contents calculated from model are compared with that from experiment. It can be seen from the figures that the model can be used to predict the chloride binding capacity of cement pastes and cement fly-ash pastes at various curing time and chloride exposure period up to a certain satisfactory degree.

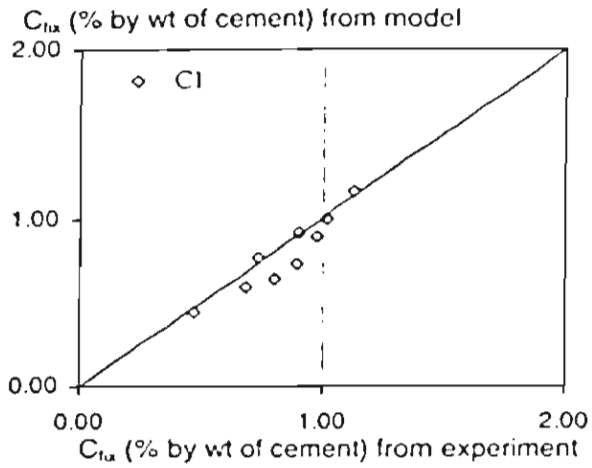

Fig. 8 Verification of model with cement paste

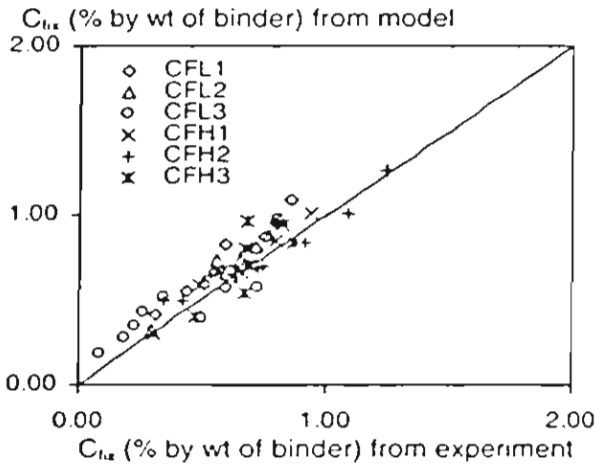

Fig. 9 Verification of model with various cement-fly ash pastes

6. Conclusions

Based on the experimental results, the model formation and the verification of model, the following conclusions can be drawn.

1. The behavior of chloride binding capacity of cement-fly ash pastes was time-dependent. Chloride binding depended on the curing and chloride exposure periods. Pastes having older age prior to chloride attack bound less amount of chloride than those exposed to chloride at younger age. Longer exposure period of paste resulted in larger content of bound chloride.
2. Cement pastes with high calcium fly ash had higher fixed chloride content than those with low calcium fly ash. This is because high calcium fly ash usually contains some cementitious components which can hydrate to bind chloride and also to increase the early pozzolanic reaction so that higher products from fly ash reactions can be produced especially at the high replacement ratio
3. A model for predicting chloride binding capacity of cement-fly ash pastes was proposed by considering that the unhydrated aluminate (C_3A) and aluminoferrite (C_4AF) phases in cement were considered responsible for the chemical binding, while the hydrated products from cement and pozzolanic products from fly ash were responsible for physical binding. The model can satisfactorily predict the chloride binding capacity of cement paste and cement-fly ash pastes with different mixture proportion, properties of fly ash, curing time and chloride exposure period.

Acknowledgements

The authors gratefully acknowledge the support provided for this research by the Thailand Research Fund (TRF).

References

[1] Arya C., Buenfeld N.R., Newman J.B., 'Factors influencing chloride-binding in concrete', *Cement and Concrete Research*, 1990, 291-300

[2] Suryavanshi A.K., Scantlebury J.D., Lyon S.B., 'The binding of chloride ions by sulphate resistant Portland cement', *Cement and Concrete Research*, 1995, 581-592

[3] Dhir R.K., El-Mohr M.A.K., Dyer T.D., 'Chloride Binding in GGBS concrete', *Cement and Concrete Research*, 1996, 1767-1773

[4] Nipatsat, N., Tangtermsirikul S., 'Compressive strength prediction model for fly ash concrete', *Thammasat International Journal of Science and Technology*, 2000, 1-7

[5] Tangtermsirikul S., Tatong, S., 'Modeling of aggregate stiffness and its effects on shrinkage of concrete', *Science Asia*, 2001, 185-192

3.2 สมนึก ตั้งเติมสิริกุล, การเคลื่อนที่ของคลอไรด์ในคอนกรีตและการเกิดสนิมในเหล็ก, การบรรยายพิเศษเรื่อง ความคงทนของคอนกรีตและโครงสร้างชายทะเล, 5 กันยายน 2545, ณ คณะวิศวกรรมศาสตร์ จุฬาลงกรณ์มหาวิทยาลัย จัดโดยคณะวิศวกรรมศาสตร์ จุฬาลงกรณ์มหาวิทยาลัย ร่วมกับคณะอนุกรรมการสาขาคอนกรีตและวัสดุวิศวกรรมสถานแห่งประเทศไทย ในพระบรมราชูปถัมภ์

(เอกสารประกอบการบรรยายไม่มี เนื่องจากใช้เป็นสไลด์ POWERPOINT)

3.3 T. Sumranwanich and S. Tangtermsirikul, A chloride binding capacity model for cement-fly ash binder taking into account the time-dependent effect, The 8th National Convention on Civil Engineering, Khon Kaen, Thailand, October 23-25, 2002

A chloride binding capacity model for cement-fly ash binder taking into account the time-dependent effect

T. Sumranwanich & S. Tangtermsirikul
Sirindhorn International Institute of Technology, Thammasat University, Pathum Thani, Thailand

ABSTRACT: This paper presents a model for predicting time-dependent chloride binding capacity of cement-fly ash binder. The proposed model took into account both chemical binding and physical binding. Chemical binding was considered to depend on the amount of unhydrated aluminate and aluminoferrite phases while physical binding depended upon the quantity of hydrated and pozzolanic products. The concept of time-dependent chloride binding capacity was introduced in the model with the consideration of curing time and chloride exposure period. The chloride bindings of cement pastes and cement-fly ash pastes under different curing time and chloride exposure period were tested. The experimental results showed that the chloride binding capacity depends on many factors, such as cement and fly ash types, fly ash content, curing time prior to chloride attack and chloride exposure period. The analytical results from model were verified with the experimental results. The verification showed that the proposed model is satisfactory for predicting the chloride binding capacity of various cement-fly ash binders.

KEYWORDS: CHLORIDE BINDING, TIME-DEPENDENT, FLY ASH, CORROSION, CHLORIDE

1 INTRODUCTION

One of the predominant causes of the corrosion of steel in concrete is chloride attack. Chloride ions may be present in concrete mixture, either as a result of using contaminated ingredients or some chemical admixtures or as a result of penetration from external sources such as seawater or de-icing salts. Only free chlorides present in pore solution can initiate corrosion when the free chloride content around the steel reaches a critical value. Therefore, the ability of hydrating cement to bind chlorides from the pore solution in concrete is an important factor which controls the initiation of chloride-induced corrosion of steel in concrete.

Chloride binding capacity of various cementitious pastes had been studied by many researchers. Some proposed a model for predicting the chloride binding capacity of cement-ground granulated blastfurnace slag paste [Dhir et al. 1996]. However, there is still no model that considers the effect of curing time and chloride exposure period in the prediction of chloride binding capacity of cement-fly ash paste.

Aluminate (C_3A) and aluminoferrite (C_4AF) phases in cement were found to be responsible for the chemical binding of chloride [Rasheeduzzafar et al. 1991, Suryavanshi et al. 1995, Csizmadia et al. 2001]. These two phases form Friedel's salt ($Ca_6Al_2O_6.CaCl_2.10H_2O$) and calcium chloroferrite ($Ca_6Fe_2O_6.CaCl_2.10H_2O$). Hussain et al. (1994) found that the increase of sulfate content in cement was found to reduce the chloride binding capacity since sulfates were stronger bound with C_3A than chlorides. Jensen et al. (2000) showed that the contents of C_3A, C_4AF and sulfate in cement were significant parameters influencing the chemical binding of chloride. While chemical binding was discovered to depend on the content of aluminate and aluminoferrite phases in cement, physical binding depended upon the content of hydrated products, particularly the content of C-S-H in concrete [Luping et al. 1993 and Delagrave et al. 1997]. Moreover, Jensen and Pratt (1989) found that calcium aluminate hydrates produced by the pozzolanic reaction of fly ash cement blends can bind the chloride.

The aim of this study is to propose a model for predicting chloride binding capacity of cement-fly ash cementitious system based on mixture proportion and properties of cementitious materials. The time-dependent effects of curing time prior to chloride attack and chloride exposure period on the chloride binding capacity were considered in the model. Both chemical binding and physical binding were included into the model. The validity of the model was verified by the experimental results.

2 EXPERIMENTAL PROGRAM

2.1 Materials, mix proportion and specimen preparation

Two types of cement, which were type I and type V Portland cements, have been used in this study. Two types of fly ash corresponding to ASTM F-type (low calcium fly ash) and ASTM C-type (high calcium fly ash) were mixed with type I Portland cement for producing the cement-fly ash pastes. The chemical composition and physical properties of cement and fly ash are listed in Table 1.

Table 1. Chemical composition and physical properties of Portland cement and fly ash

Chemical composition	Cement		Fly ash	
	I	V	Class F	Class C
SiO_2 (%)	20.61	20.97	45.55	38.42
Al_2O_3 (%)	5.03	3.49	26.20	19.17
Fe_2O_3 (%)	3.03	4.34	10.94	10.93
CaO (%)	64.89	62.86	8.28	17.28
MgO (%)	1.43	3.33	2.83	7.95
SO_3 (%)	2.70	2.12	1.04	2.01
Na_2O(%)	0.22	0.12	0.90	1.03
K_2O (%)	0.46	0.47	2.78	2.28
Free lime (%)	0.79	1.01	-	-
LOI (%)	1.23	1.21	0.17	0.05
Blaine fineness (cm^2/g)	3,190	3,760	3,460	3,510
Bogue's potential compound composition				
C_3S (%)	61.64	60.77		
C_2S (%)	12.68	14.37		
C_3A (%)	8.21	1.91		
C_4AF (%)	9.21	13.19		

Eight different mixture conditions of cementitious paste were prepared for this investigation, as shown in Table 2. There were two mixture conditions of cement paste and six mixture conditions of cement-fly ash paste.

Table 2. Mixture conditions

Mix	Materials		w/b	f/b	Curing	Exposure
	Cement	Fly ash			time (day)	period (day)
C1	Type I	-	0.40	-	1, 7, 28	28, 56, 91
C2	Type V	-	0.40	-	1, 7, 28	28, 56, 91
CFL1	Type I	F*	0.40	0.30	1, 7, 28	28, 56, 91
CFL2	Type I	F*	0.40	0.50	1, 7, 28	28, 56, 91
CFL3	Type I	F*	0.40	0.70	1, 7, 28	28, 56, 91
CFH1	Type I	C**	0.40	0.30	1, 7, 28	28, 56, 91
CFH2	Type I	C**	0.40	0.50	1, 7, 28	28, 56, 91
CFH3	Type I	C**	0.40	0.70	1, 7, 28	28, 56, 91

*F-type fly ash has (SiO_2+Al_2O_3+Fe_2O_3) content greater than 70% and is called as *low calcium fly ash* in this study.
**C-type fly ash has (SiO_2+Al_2O_3+Fe_2O_3) content less than 70% and is called as *high calcium fly ash* in this study.

In order to achieve rapid saturation, thin disc specimens of 50 mm diameter and 10 mm thick cast in PVC molds were selected for sample preparation. Thirteen specimens were prepared for each mixture condition, ten for expressing the pore solution and three for determining the evaporable water content. The mixing procedure was performed according to ASTM C305.

2.2 Curing time and chloride exposure period

After casting, specimens were sealed with plastic sheet to prevent drying for 24 hours. Except for specimens to be exposed to chloride at 1 day, all specimens were cured in water immediately after removal from the molds. Curing times were 1, 7 and 28 days as shown in Table 2. The curing temperature was 30±2°C.

At the end of water curing, specimens were exposed to chloride by submerging in salt water with 3.0 % of chloride ion concentration (30 gram per liter) for different exposure periods. The exposure periods were 28, 56 and 91 days as shown in Table 2. The volume of salt water (chloride solution) was 2.0 liters. The temperature during the chloride exposure period was 30±2°C.

2.3 Determination of chloride content

At the end of chloride exposure period, specimens were removed from salt water. Surfaces of specimen were dried by using tissue paper. Pore solution inside the specimens was obtained by using a pore pressing apparatus. The maximum loading pressure for expressing the pore solution was about 500 MPa. Two or three cycles of loading and unloading were performed in order to get 3 to 5 cm^3 of pore solution. The evaporable water content of specimen was immediately tested for being used in the determination of free chloride in the specimen.

Total chloride content was determined from the difference between initial chloride content of the submerging salt water at the start of exposure and its final chloride content at the end of exposure and shared equally to all specimens submerged in the salt water. The free chloride content was determined from chloride concentration of pore solution pressed from specimen multiplied with the evaporable water. Finally, the fixed chloride content of cementitious paste can be determined by subtracting the total chloride content with the free chloride content. All chloride concentrations were analyzed by potentiometric titration with $AgNO_3$ solution and chloride ion selective electrode.

3 CHLORIDE BINDING CAPACITY MODEL

The chloride binding capacity model of cement-fly ash cementitious system considering both chemical and physical bindings is given in Eq. 1.

$$C_{fix}(t_s, t_e) = C_{fix,\,chem}(t_s, t_e) + C_{fix,\,phy}(t_e) \quad (1)$$

where $C_{fix}(t_s, t_e)$ is the total fixed chloride content in the cementitious system (% by weight of binder), $C_{fix,\,chem}(t_s, t_e)$ is the fixed chloride content by chemical binding (% by weight of binder), $C_{fix,\,phy}(t_e)$ is the fixed chloride content by physical binding (% by weight of binder), t_s is the age at the start of chloride exposure which is equal to curing time and t_e is the age at the end of chloride exposure. It is noted that t_e- t_s means the chloride exposure period.

3.1 Hydrated mass of cement and reacted mass of fly ash

The mass of each major compound in Portland cement was calculated based upon Bogue's equation. The hydrated mass of compound i at age t was determined from Eq. 2.

$$M_{hyd,\,i}(t) = (M_i \,.\, \alpha_i) / 100 \quad (2)$$

where $M_{hyd,\,i}(t)$ is the hydrated mass of compound i at age t days (kg/m^3 of concrete), M_i, is the mass of each major compound in Portland cement (kg/m^3 of concrete), $\alpha_i(t)$ is the degree of hydration of compound i of cement at age t days (%) and t is the age of the sample (day).

The reacted mass of fly ash in the pozzolanic reaction at age t days was calculated according to Eq. 3.

$$M_{poz,\,fa}(t) = (M_{fa} \,.\, \alpha_{fa}) / 100 \quad (3)$$

where $M_{poz,\,fa}(t)$ is the reacted mass of fly ash at age t days (kg/m^3 of concrete), M_{fa} is the mass of fly ash (kg/m^3 of concrete) and $\alpha_{fa}(t)$ is degree of pozzolanic reaction of fly ash at age t days (%).

3.2 Hydration products and pozzolanic products

It is assumed here for simplicity that the quantity of hydrated products of cement and pozzolanic products of fly ash are determined based on the reactions shown in Table 3. The quantity of products is calculated based on the reaction equations in that table and their corresponding hydrated mass of cement and reacted mass of fly ash.

Table 3. Reactions of cement and fly ash [Mindess 1981]

Cement	Reactions
C_3A	$2C_3A + 3C\underline{S}H_2 + 26H \rightarrow C_6A\underline{S}_3H_{32}$
	$2C_3A + C_6A\underline{S}_3H_{32} + 4H \rightarrow 3C_4A\underline{S}H_{12}$
	$C_3A + 6H \rightarrow C_3AH_6$
C_4AF	$C_4AF + 3C\underline{S}H_2 + 21H \rightarrow C_6(A,F)\underline{S}_3H_{32} + (A,F)H_3$
	$2C_4AF + C_6(A,F)\underline{S}_3H_{32} + 7H \rightarrow C_4(A,F)\underline{S}H_{12} + (A,F)H_3$
	$C_4AF + 9H + 4CH \rightarrow C_4(A,F)H_{13}$
C_3S	$2C_3S + 6H \rightarrow C_3S_2H_3 + 3CH$
C_2S	$2C_2S + 4H \rightarrow C_3S_2H_3 + CH$
Fly ash	**Reactions**
S	$2S + 3CH \rightarrow C_3S_2H_3$
A	$2A + 3CH \rightarrow C_3A_2H_3$

C = CaO, S = SiO_2, A = Al_2O_3, F = Fe_2O_3, H = H_2O, $\underline{S}$ = SO_3

3.3 Chemical binding

In general, a part of C_3A and C_4AF in cement firstly react with gypsum to form ettringite and monosulfate. Afterwards, the rest of unhydrated C_3A and C_4AF react further with water during curing period. It is considered that only some fractions of original content of C_3A and C_4AF are efficient for chemical binding. The efficient parts are those react during the chloride exposure period only and form Friedel's salt and calcium chloroferrite whereas those reacted before the chloride exposure period do not contribute to chemical binding. The fixed chloride content by chemical binding, $C_{fix,\,chem}(t_s, t_e)$, is defined as shown in Eq. 4. The time-dependent effects of curing time, t_s, and age at the end of chloride exposure, t_e, were taken into account in this equation.

$$C_{fix,\,chem}(t_s, t_e) = C_{fix,\,C3A}(t_s, t_e) + C_{fix,\,C4AF}(t_s, t_e) \quad (4)$$

where $C_{fix,\,C3A}(t_s, t_e)$ and $C_{fix,\,C4AF}(t_s, t_e)$ are the fixed chloride contents by chemical binding of C_3A and C_4AF, respectively during the exposure period.

The amount of $C_{fix,\,C3A}(t_s, t_e)$ and $C_{fix,\,C4AF}(t_s, t_e)$ can be determined from Eq. 5 and Eq. 6, respectively.

$$C_{fix,C3A}(t_s, t_e) = \lambda_{fix,C3A} \cdot [M_{hyd,C3A}(t_e) - M_{hyd,C3A}(t_s)] \quad (5)$$

$$C_{fix,C4AF}(t_s, t_e) = \lambda_{fix,C4AF} \cdot [M_{hyd,C4AF}(t_e) - M_{hyd,C4AF}(t_s)] \quad (6)$$

in which

$$\lambda_{fix,C3A} = \frac{1.12}{3.3 + e^{(0.03 \times \Delta\alpha_{C3A})}} \quad (7)$$

and

$$\lambda_{fix,C4AF} = \frac{0.6}{3.3 + e^{(0.033 \times \Delta\alpha_{C4AF})}} \quad (8)$$

where $\lambda_{fix,\,C3A}$ and $\lambda_{fix,\,C4AF}$ are defined as the fixed chloride ratios of C_3A and C_4AF, i.e., the ratios of fixed chloride to hydrated mass of C_3A and C_4AF, respectively, and $\Delta\alpha_{C3A}$ and $\Delta\alpha_{C4AF}$ are the changes of degree of hydration of C_3A and C_4AF, respectively during the exposure period.

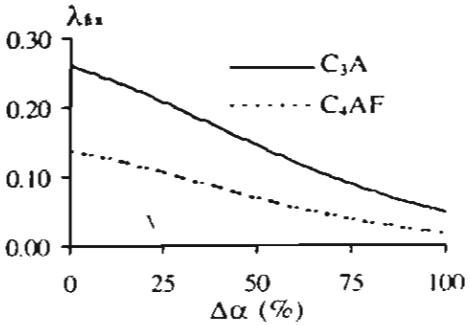

Figure 1. Relationship between fixed chloride ratios of C_3A and C_4AF and change of degree of hydration during the exposure period

The relationship between the fixed chloride ratios of C_3A and C_4AF and their respective changes of degree of hydration are shown in Fig. 1. The fixed chloride ratio decreases with the increase of the change of degree of hydration reaction during exposure period. This implies that more chloride can chemically be bound at early hydrations of C_3A and C_4AF.

3.4 Physical binding

Chloride may be physically adsorbed on the surface of C-S-H gel and other products of reactions in cementitious system, such as C-A-H, C-A-F-H, ettringite and monosulfate. The fixed chloride content by physical binding at the end of chloride exposure, $C_{fix,\,phy}(t_e)$, is defined as in Eq. 9. This equation also takes into account the time-dependent effect of curing time plus chloride exposure period, t_e.

$$C_{fix,\,phy}(t_e) = (\Sigma M_{product}(t_e) \cdot \phi_{fix}) / 100 \qquad (9)$$

where ϕ_{fix} is the fixed chloride content of hydrated and pozzolanic products (%) and $\Sigma M_{product}(t_e)$ is the summation of mass of hydrated products and pozzolanic products at the end of chloride exposure.

For simplicity, it is assumed here that all hydrated and pozzolanic products have the same fixed chloride content. The fixed chloride content of hydrated and pozzolanic products depends on the total chloride content, water to binder ratio and fineness of cement in the cementitious system. The physically bound chloride content was derived from the back computation using test data of chloride binding capacity. The derived equation is shown in Eq. 10.

$$\phi_{fix} = \left(\frac{-0.093 \times w/b + 0.135}{0.037 + e^{(-0.0002 \times w/b^{(-4.89)}) - 1.572) C_{tot}}} \right) \times \left(\frac{C_{tot}}{C_{tot} + 0.01} \right) \times \left(\frac{F_c}{3190} \right)^{0.5} \qquad (10)$$

where C_{tot} is the total chloride content (% by weight of binder), w/b is the water to binder ratio and F_c is the Blaine fineness of cement (cm^2/g)

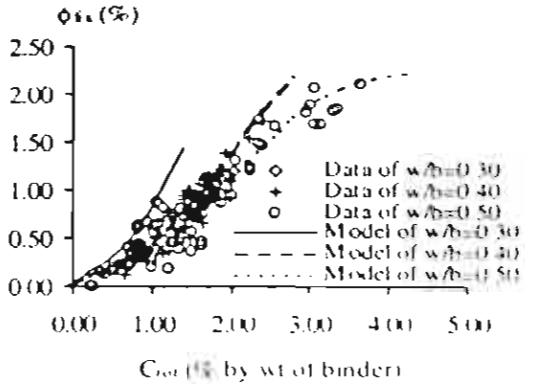

Figure 2. Fixed chloride content for hydrated and pozzolanic products

As shown in Fig. 2, the physically bound chloride content of hydrated and pozzolanic products increases with increasing total chloride content and decreasing water to binder ratio.

4 RESULTS AND DISCUSSIONS

The test results of total chloride and fixed chloride are presented by bar charts. The values in parentheses above the bar indicate the ratios of fixed chloride content to total chloride content.

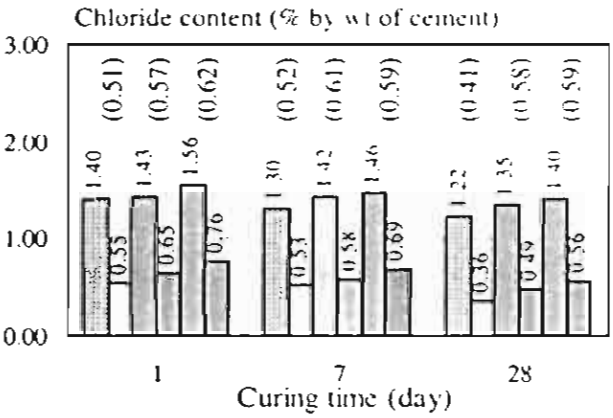

(a) Type I cement

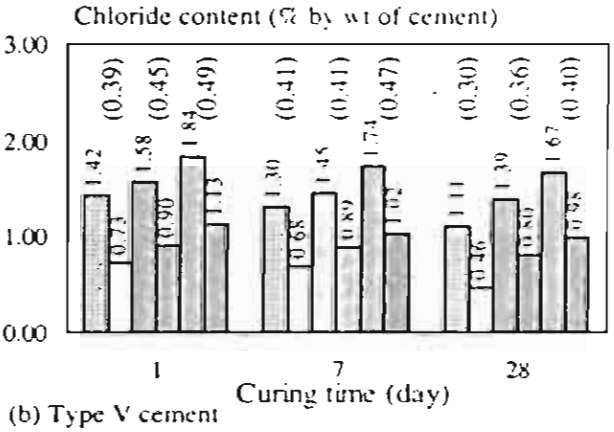

(b) Type V cement

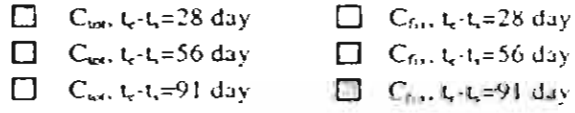

Figure 3. Chloride binding capacity of cement paste

It can be seen from Fig. 3 that the chloride binding capacity of cement paste exhibits a time dependent behavior. Considering samples with the same exposure period, t_e-t_s, paste with shorter curing time had higher total and fixed chloride content than that with longer one. The reason for larger total chloride content in shorter curing time case was that younger paste had bigger pore diameter, so larger amount of chloride can penetrate into the paste. Fixed chloride was also higher because there were larger amount of unhydrated aluminate and aluminoferrite phases, which were accessible for chloride binding.

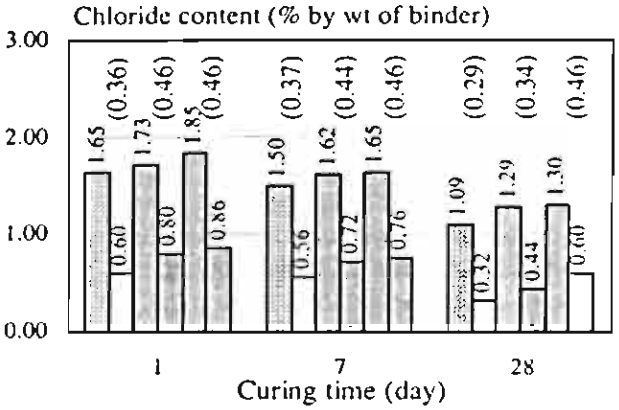

(a) Fly ash to binder ratio (f/b) = 0.30

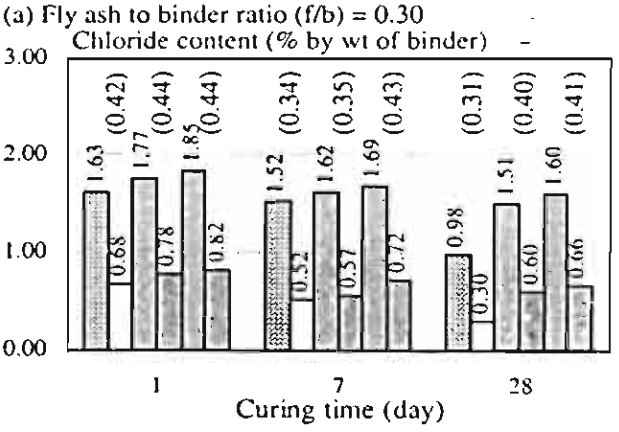

(b) Fly ash to binder ratio (f/b) = 0.50

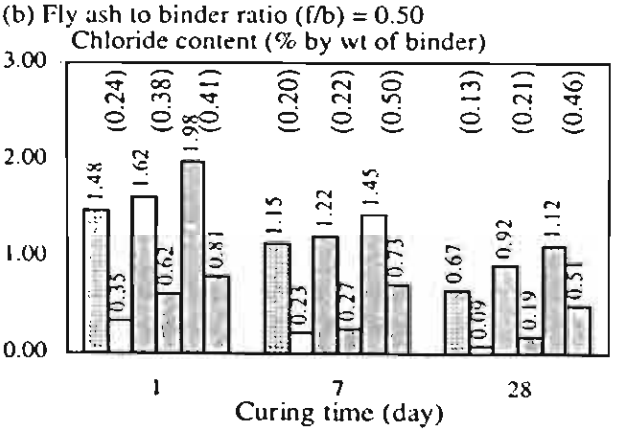

(c) Fly ash to binder ratio (f/b) = 0.70

□ C_{tot}, t_e-t_s=28 day □ C_{fix}, t_e-t_s=28 day
□ C_{tot}, t_e-t_s=56 day ■ C_{fix}, t_e-t_s=56 day
□ C_{tot}, t_e-t_s=91 day ■ C_{fix}, t_e-t_s=91 day

Figure 4. Chloride binding capacity of type I cement - low calcium fly ash paste

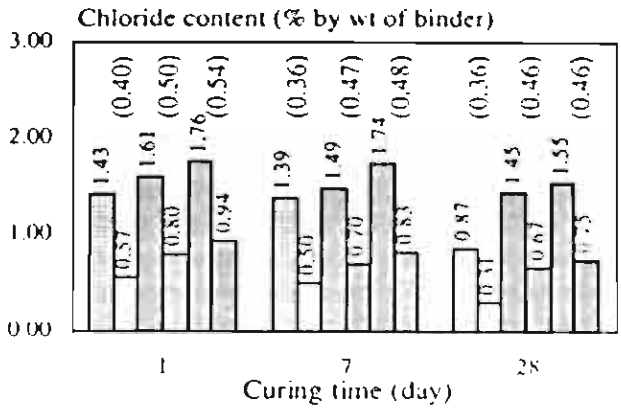

(a) Fly ash to binder ratio (f/b) = 0.30

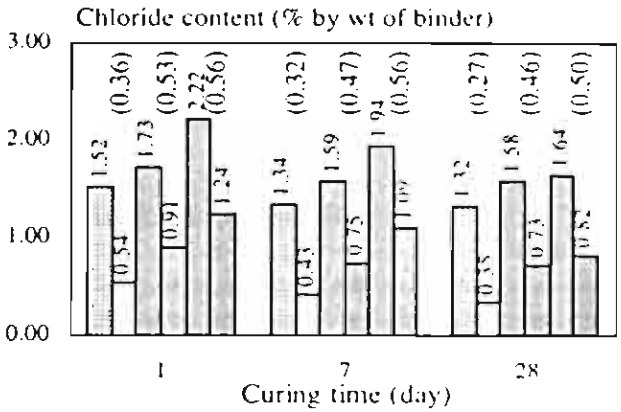

(b) Fly ash to binder ratio (f/b) = 0.50

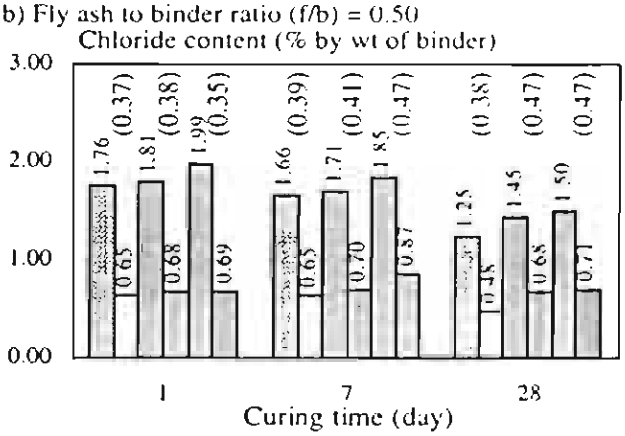

(c) Fly ash to binder ratio (f/b) = 0.70

□ C_{tot}, t_e-t_s=28 day □ C_{fix}, t_e-t_s=28 day
□ C_{tot}, t_e-t_s=56 day □ C_{fix}, t_e-t_s=56 day
□ C_{tot}, t_e-t_s=91 day □ C_{fix}, t_e-t_s=91 day

Figure 5. Chloride binding capacity of type I cement - high calcium fly ash paste

On the contrary, considering pastes with the same curing time, longer exposure period in saltwater resulted in higher total and fixed chloride content. Higher total chloride was due to longer exposure period while the reason for larger fixed chloride content was that larger amount of hydrated and pozzolanic products produced during the longer exposure period can bind chlorides.

When comparing Fig. 3(a) with Fig. 3(b), it can be observed clearly that type V cement paste had lower fixed chloride content than type I cement paste for all curing and exposure periods. This was

mainly because the type V cement had lower content of C_3A than type I cement.

In addition, Fig. 4 and Fig. 5 show that the characteristics of time-dependent chloride binding of cement-fly ash paste follow the same trend as those of the cement paste.

Fig. 4 and Fig. 5 illustrate that cement paste with high calcium fly ash had higher fixed chloride content than that with low calcium fly ash. This is because the high calcium fly ash usually contains some cementitious components which can hydrate to bind chloride and also to increase the early pozzolanic reaction so that higher pozzolanic products can be produced especially at the high replacement ratio.

5 VERIFICATION

Fig. 6 shows the verification of model with the experimental results conducted by the authors. In the figure, the fixed chloride contents calculated from model are compared with those from experiment. It can be seen that the model can be used to predict the chloride binding capacity of cement pastes and cement fly-ash pastes under various curing time and chloride exposure period with satisfactory accuracy.

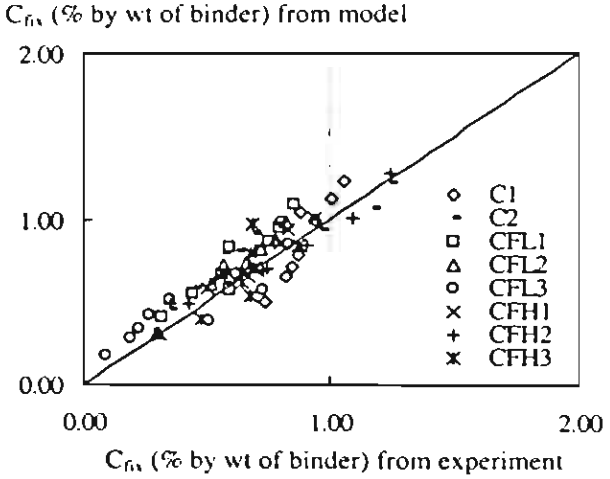

Figure 6. Verification of chloride binding capacity model

6 CONCLUSIONS

Based on the test results and the purposed model, the following conclusions can be drawn.

1. The behavior of chloride binding capacity of cement-fly ash cementitious system was time-dependent. Chloride binding depended on curing and chloride exposure periods. Pastes having older age prior to chloride attack bound less chloride than those exposed to chloride at younger age. Longer exposure period of paste resulted in larger chloride binding capacity.
2. Cement paste with high calcium fly ash had higher fixed chloride content than that with low calcium fly ash. This is because the high calcium fly ash usually contains some cementitious components which can hydrate to bind chloride and also to increase the pozzolanic reaction so that higher pozzolanic products can be produced especially the high replacement ratio
3. A model for predicting chloride binding capacity of cement-fly ash binder was proposed by considering that the unhydrated aluminate (C_3A) and aluminoferrite (C_4AF) phases in cement were considered responsible for the chemical binding, while the hydrated products from cement and pozzolanic products from fly ash were responsible for physical binding.
4. The proposed model can satisfactorily predict the chloride binding capacity of various cement pastes and cement-fly ash pastes with different mixture proportion, properties of cement and fly ash, curing time and chloride exposure period.

ACKNOWLEDGEMENTS

The authors gratefully acknowledge the support provided for this research by the Thailand Research Fund (TRF).

REFERENCES

Csizmadia J., Balazs G., Tamas F.D., 2001 'Chloride ion binding capacity of aluminoferrites', *Cement and Concrete Research* 31: 577-588

Delagrave A., Marchand J., Ollivier J.P., Julien S., Hazrati K., 1997 'Chloride binding capacity of various hydrated cement paste systems', *Advanced Cement Based Materials* 6: 28-35

Dhir R.K., El-Mohr M.A.K., Dyer T.D., 1996 'Chloride Binding in GGBS concrete', *Cement and Concrete Research* 26: 1767-1773

Hussain E.S., Rasheeduzzafar, Al-Gahtani A.S., 1994 'Influence of sulfates on chloride binding in cements', *Cement and Concrete Research* 24: 8-24

Jensen H.-U., Pratt P.L., 1989 'The binding of chloride ions by pozzolanic product in fly ash cement blends', *Advances in Cement Research* 2: 121-129

Jensen O.M., Korzen M.S.H., Jakobsen H.J., Skibsted J., 2000 'Influence of cement constitution and temperature on chloride binding in cement paste', *Advances in Cement Research* 12: 57-64

Luping, T. & Nilsson L.-O., 1993 'Chloride binding capacity and binding isotherms of OPC pastes and mortars', *Cement and Concrete Research* 23: 247-253

Mindess S., Young J.F., 1981 'Concrete', Prentice-Hall, New Jersey

Rasheeduzzafar, Hussain E.S., Al-Saadoun S.S., 1991 'Effect of cement composition on chloride binding and corrosion of reinforcing steel in concrete', *Cement and Concrete Research* 21: 777-794

Suryavanshi A.K., Scantlebury J.D., Lyon S.B., 1995 'The binding of chloride ions by sulphate resistant Portland cement', *Cement and Concrete Research* 25: 581-592

For further details, contact Assoc. Prof. Dr. Somnuk Tangtermsirikul, tel. 0-2986-9009 ext. 1908, fax. 0-2986-9112 or e-mail to somnuk@sit.to.ac.th